The evolutionarily conserved protein CG9186 is associated with lipid droplets, required for their positioning and for fat storage

Katharina Thiel[1], Christoph Heier[2], Verena Haberl[2], Peter J. Thul[1,3], Monika Oberer[2], Achim Lass[2], Herbert Jäckle[1] and Mathias Beller[1,3,*]

[1]Department of Molecular Developmental Biology, Max Planck Institute for Biophysical Chemistry, Göttingen, Germany
[2]Institute of Molecular Biosciences, University of Graz, Graz, Austria
[3]Institute for Mathematical Modeling of Biological Systems, Heinrich Heine University Düsseldorf, Düsseldorf, Germany
*Author for correspondence (mathias.beller@hhu.de)

Summary

Lipid droplets (LDs) are specialized cell organelles for the storage of energy-rich lipids. Although lipid storage is a conserved feature of all cells and organisms, little is known about fundamental aspects of the cell biology of LDs, including their biogenesis, structural assembly and subcellular positioning, and the regulation of organismic energy homeostasis. We identified a novel LD-associated protein family, represented by the *Drosophila* protein CG9186 and its murine homolog MGI:1916082. In the absence of LDs, both proteins localize at the endoplasmic reticulum (ER). Upon lipid storage induction, they translocate to LDs using an evolutionarily conserved targeting mechanism that acts through a 60-amino-acid targeting motif in the center of the CG9186 protein. Overexpression of CG9186, and MGI:1916082, causes clustering of LDs in both tissue culture and salivary gland cells, whereas RNAi knockdown of CG9186 results in a reduction of LDs. Organismal RNAi knockdown of CG9186 results in a reduction in lipid storage levels of the fly. The results indicate that we identified the first members of a novel and evolutionarily conserved family of lipid storage regulators, which are also required to properly position LDs within cells.

Key words: Lipid droplets, Organelle clustering, Organelle positioning, Lipid metabolism, *Drosophila melanogaster*

Introduction

The storage of lipids as a reservoir for energy rich compounds and metabolic building blocks is important for individuals of all kingdoms of life. Storage amounts are usually kept constant at intermediate levels. This is achieved by a rapid and dynamic response to fluctuations in nutritional status and energy demands causing a storage amount increase or remobilization, respectively. Deregulation of this process, called energy homeostasis, has severe consequences for the organism as seen in emerging human metabolic diseases such as lipodystrophies or obesity.

On the cellular level, lipids are stored in specialized functional units, the lipid droplets (LDs), which were only recently acknowledged as organelles. All LDs share a simple and stereotyped structure. They are composed of a hydrophobic core of stored lipids surrounded by a phospholipid hemimembrane with proteins attached (reviewed by Farese and Walther, 2009).

LDs are thought to emerge at the cytoplasmic leaflet of the endoplasmic reticulum (ER) membrane by a budding like process. Mechanistic details as well as the machinery involved in this process are still unknown. However, at least some members of the LD-associated proteome are known to target to LDs via the ER (Horiguchi et al., 2008; Zehmer et al., 2009) and might thus be involved in LD biogenesis or mark the sites of LD biogenesis. Once LDs are released into the cytosol, their positioning within the cell as well as their sizes are adjusted in response to the cellular nutritional status and the energy demands of the organism.

LD positioning and size appears to be governed by the LD surfactant properties, i.e. their protein and phospholipid composition (reviewed by Yang et al., 2012). For example, proteins of the PERILIPIN family (also known as the PAT protein family) (Bickel et al., 2009; Kimmel et al., 2010) seem to play a direct role in LD size regulation, since organismic PERILIPIN loss-of-function mutations (Beller et al., 2010) or the simultaneous RNAi-mediated knockdown of partially redundant PERILIPINs in cells (Bell et al., 2008) results in giant LDs. Whether the observed size changes are based on a fusion of pre-existing LDs or on a preferential growth of given LDs has not yet been established. The prevalence and importance of LD fusion for size expansion is under debate (Boström et al., 2007; Murphy et al., 2010). A prerequisite for LD fusion is close apposition (clustering). Clustering, however, is not sufficient to induce LD fusion, since in certain cell lines such as *Drosophila* S2 (Guo et al., 2008) or human A431 cells (Hynynen et al., 2009) clustered LDs are the default state. The mechanisms used to position LDs within cells are poorly understood and only few proteins are known to affect LD positioning. An example is Fld1p/Seipin, whose mutation results in a clustering of LDs in yeast and mammalian cells (Fei et al., 2008; Szymanski et al., 2007; Tian et al., 2011) and causes the Berardinelli–Seip congenital lipodystrophy in humans (Magré et al., 2001). Not

only loss-of-function mutations, but also overexpression can result in a clustering of LDs in cells as demonstrated for the Fsp27/cidec (Nishino et al., 2008) or Hepatitis C Virus core protein (Boulant et al., 2008). The mechanistic details underlying the clustering phenotypes are not yet fully understood. For Fsp27/cidec an altered flow of lipids between neighboring LDs (Gong et al., 2011) might explain the clustering. In Seipin mutants, LDs appear to bud uncontrolled from the ER (Szymanski et al., 2007).

Besides LD regulatory proteins, recent data also demonstrate the importance of the LD phospholipid composition for the positioning and size control of LDs. The phosphatidylcholine content of the LD phospholipid monolayer membrane has been proposed to be critical for LD size regulation (Fei et al., 2011a; Krahmer et al., 2011). Since most of the neutral and phospholipid synthesis machinery enzymes are localized to the ER, this compartment clearly plays an important role in LD biogenesis and size regulation. Recent reports additionally demonstrated the presence and activity of lipogenic enzymes at the LD surface, suggesting a secondary editing and modulation of lipid amounts after the LD release from the ER (Digel et al., 2009; Krahmer et al., 2011; Kuerschner et al., 2008). Since the dispersion and clustering of LDs was linked to LD growth and remobilization as well as lipolytic accessibility (Nishino et al., 2008) a better understanding of the regulatory and mechanistic events of this process are important.

Here we present a detailed analysis of a novel LD-associated protein, CG9186, which we identified in a previous proteomics screen with *Drosophila melanogaster* third instar larval fat body LDs (Beller et al., 2006). We show that CG9186 is a member of a novel and uncharacterized but evolutionarily well conserved protein family which has an annotated esterase/lipase domain in common. In agreement with its role in lipid metabolism, overexpressed and endogenous CG9186 decorates LDs both in fly tissue culture cells and in the lipid storage tissues of the organism. The murine homolog of CG9186, termed MGI:1916082, also targets to LDs in tissue culture cells. Overexpression of the fly and mouse proteins results in a clustering of LDs, showing their function in LD positioning as opposed to a function in LD remobilization. Structure-function experiments revealed that both the predicted catalytic center and the C-terminal part of the protein is important for LD clustering. Conversely, knockdown of CG9186 encoding transcripts causes decreased lipid storage levels in the organism. In summary, CG9186 is the first identified member of an evolutionarily conserved family of lipid storage regulating proteins which is important for both LD biogenesis and positioning.

Results
The LD-associated protein CG9186 belongs to an evolutionarily conserved family of putative lipases
CG9186 was identified in previous proteomics screens geared to detect LD resident proteins of *Drosophila* third instar larval fat bodies (Beller et al., 2006) and embryos (Cermelli et al., 2006). The protein belongs to a family of annotated lipases with representatives in all phyla (Fig. 1A,B). In *Drosophila*, the CG9186 gene locus is located on the left arm of chromosome 3 at position 61F6 (Fig. 1C) according to the FlyBase version FB2012_06 annotation (McQuilton et al., 2012). Two transcript variants are described: CG9186-RA and -RB. They differ in their 5′ untranslated region but otherwise result in the same 307 amino acid polypeptide sequence which lacks obvious functional protein

domains except for a well conserved lipase motif (EC 3.1.1.3). The motif is marked by a central serine at amino acid position 119 which is conserved in all sequences investigated (Fig. 1B). Together with conserved aspartate and histidine residues at positions 254 and 283, this serine potentially forms a complete catalytic triad that is characteristic for functional lipase enzymes (Jaeger et al., 1999). Based on homology modeling, we found that the three residues likely come to sufficient close spatial arrangement (Fig. 1D) to act cooperatively in a catalytic reaction.

Whole mount *in situ* hybridizations with antisense RNA probes showed that the CG9186 encoding transcripts are maternally provided and later on presumably restricted to the salivary glands (Fig. 1E). Salivary gland expression was confirmed by combining a fluorescent *in situ* detection of CG9186 transcripts with an antibody staining for the salivary gland marker protein crebA (Fox et al., 2010) (Fig. 1F). Earlier microarray (www.flyatlas.org) (Chintapalli et al., 2007) and RNaseq data (Celniker et al., 2009) report that CG9186 is expressed during all post-embryonic stages as well as in various tissue culture cell lines. Postembryonic expression is particularly prominent in lipid storing tissues such as the fat body or midgut, suggesting a function of CG9186 in organismic lipid storage metabolism.

In order to test the LD proteomics-based putative LD localization of CG9186, we expressed a GFP-tagged CG9186 protein variant (CG9186:eGFP) in *Drosophila* embryonic Kc167 cells (Fig. 2A). We confirmed the identity of LDs by counterstaining with the specific LD dye HCS LipidTOX Deep Red (Grandl and Schmitz, 2010) as well as co-localization with TdT-tagged PLIN2 (PLIN2:TdT), a known *Drosophila* LD-associated protein (Grönke et al., 2003; Teixeira et al., 2003; Welte et al., 2005). Fig. 2B shows that CG9186:eGFP and PLIN2:TdT colocalize at the surface of LDs. Interestingly, the LDs decorated by both proteins often appeared larger and less well rounded as compared to the non-labeled LDs (e.g. non-transfected cells in Fig. 2A). These deformed LDs could be specific for CG9186:eGFP and PLIN2:TdT co-overexpression. An alternative explanation might involve the known induction of increased lipid storage amounts by the overexpression of functional PLIN2 protein (Grönke et al., 2003) (Fig. 2E). To test this possibility we overexpressed CG9186:eGFP in cells in which the major *Drosophila* lipase gene *brummer* (Grönke et al., 2005) was targeted by RNAi or incubated the cells with 800 μM oleic acid (OA) instead of the standard 400 μM dose (Fig. 2C,D). Both conditions elevate the cellular lipid storage levels in cells (Fig. 2F,G). All tested combinations of increased lipid storage levels and CG9186:eGFP expression resulted in the enlarged and deformed LD phenotype. These results suggest that cells overexpressing CG9186 have more difficulties in properly packaging elevated storage lipid amounts.

We asked next, whether also the endogenous CG9186 protein localizes to LDs. To visualize the localization of the endogenous protein we raised specific CG9186 antisera. CG9186 decorates LDs of tissue culture cells (Fig. 3A) as well as different third instar larval tissues with endogenous CG9186 expression such as salivary glands (Fig. 3B) or fat bodies (Fig. 3C). RNAi-mediated targeting of CG9186 encoding transcripts abolished the signal (Fig. 3D) as did omission of the primary antibody (Fig. 3E). In western blots, the antibody revealed a prominent signal with a slightly smaller apparent molecular weight than the calculated 36 kDa of CG9186 (Fig. 3F). Overexpression of the CG9186:eGFP fusion protein resulted in a second signal at

around 55 kDa, which corresponded to the calculated molecular weight of the fusion protein. The detected CG9186 signal vanished, when CG9186 encoding transcripts were targeted by RNAi (Fig. 3F). Thus, the antibody is specific for CG9186 and we are able to successfully overexpress and deplete the CG9186 protein. Our results so far show that the evolutionarily conserved CG9186 protein is a bona fide LD-associated protein which may play a role in LD homeostasis.
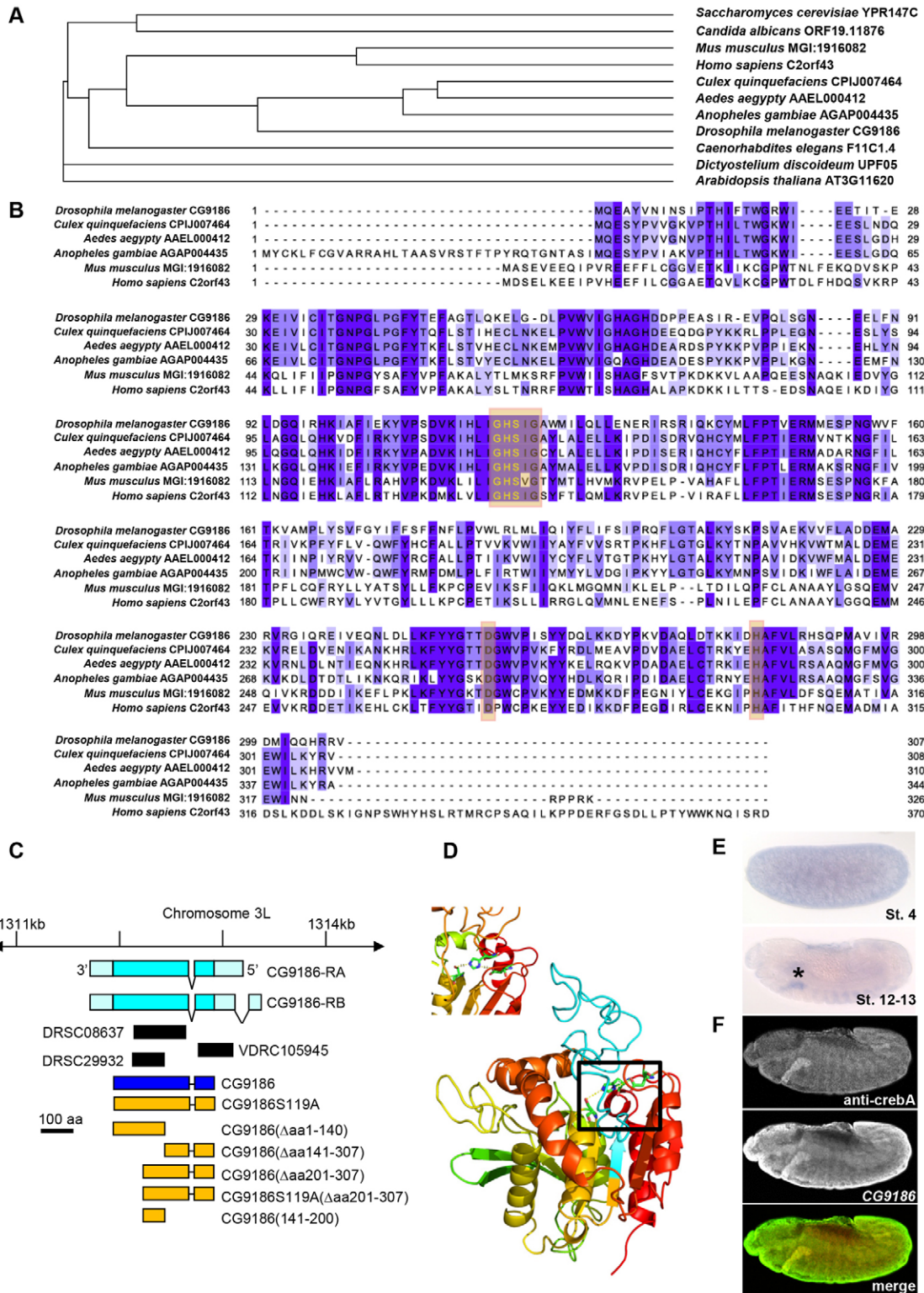

Fig. 1. See next page for legend.

CG9186 shuttles between the ER and LDs

The targeting of proteins to LDs as well as LD biogenesis per se is still poorly understood – in part because necessary tools to address these aspects of LD function are still limited (Farese and Walther, 2009; Zehmer et al., 2009). In order to assess the possibility that CG9186:eGFP may serve as such a tool we further investigated the subcellular localization of the protein. In addition to LD association, CG9186 showed a reticular localization pattern (Fig. 2A; Fig. 3A). In order to test if this second site of CG9186:eGFP localization is the ER, we employed neuronal *Drosophila* ML-DmBG3-c2 cells, which show an extensive ER network. In the absence of OA-mediated LD induction (Fig. 4A) CG9186:eGFP showed a prominent reticular distribution, which persisted following OA feeding (Fig. 4B), although it got much weaker. When we co-transfected ML-DmBG3-c2 cells with CG9186:eGFP and a TdT-tagged variant of the *Drosophila* ER lumen protein retaining receptor (KdelR:TdT; Fig. 4C) or transfected the cells with CG9186:eGFP and counterstained with the ER-Tracker Red dye (data not shown) the results showed a prominent co-localization of CG9186:eGFP and the different ER markers. Thus, CG9186:eGFP localizes in the absence of OA loading, and thus in the absence of LDs, to the ER.

In order to examine the translocation of CG9186 from the ER to LDs in OA-stimulated cells, we monitored the sub-cellular distribution of CG9186 during the course of LD biogenesis. We started with a biochemical analysis of wild-type Kc167 cells fractioned in the presence or absence of OA by discontinuous sucrose gradient ultracentrifugation (Fig. 4D), a technique suitable to separate LDs from the cytosol and cellular membranes including the ER (Beller et al., 2006). To block further protein synthesis we added cycloheximide to the growth medium. In the absence of OA very few LDs were detected in wild-type cells and accordingly only small amounts of CG9186 and PLIN2 were found in the LD fraction at the top region of the gradient (Fig. 4D). In contrast, prominent CG9186 and comparatively weaker PLIN2 protein amounts were noted in the cytosolic fraction. CG9186 was also found in the microsomal membrane fraction, where PLIN2 signal was absent (Fig. 4D). The cytoplasmic marker β-Tubulin was restricted to the cytosolic fraction and was not affected by OA addition to the growth

medium. In contrast, both CG9186 and PLIN2 protein amounts dramatically increased in the LD fraction following OA-induced LD deposition. At the same time, the other cellular CG9186 pools appeared to correspondingly decrease (Fig. 4D). These observations suggest that the CG9186 protein changes its location from the ER to LDs during OA-induced LD biogenesis.

In order to monitor the OA-induced CG9186 translocation also with temporal resolution we used time-lapse microscopy of a Kc167 cell line which stably expressed CG9186:eGFP (Fig. 4E; supplementary material Movie 1). These experiments revealed that CG9186:eGFP is first seen in a dot-like pattern about 10 minutes after OA addition which corresponds to newly formed, tiny LDs. Together with the observed shift of cellular protein pools (Fig. 4D) this observation suggests that CG9186 decorates LDs as soon as they are generated.

CG9186 overexpression results in LD clustering but no lipid mobilization phenotype

CG9186:eGFP overexpression causes clustered LDs (e.g. Fig. 2A). This phenotype is consistent with a possible role of CG9186 in the positioning of LDs within cells. In order to quantify a possible effect of overexpressed CG9186:eGFP on LD positioning, we compared the LD patterns in untransfected cells with the pattern seen in cells transiently transfected with CG9186:eGFP. Untransfected *Drosophila* Kc167 cells mainly showed dispersed LDs (93% of the cells; Fig. 5A,C) and a minority of clustered LDs (7%). In contrast, cells overexpressing CG9186:eGFP contained a significantly increased fraction of clustered LDs (51% as compared to 7% in wild-type cells; Fig. 5C).

Previous studies have shown that overexpression of lipases results in a loss of cellular triglyceride stores, as shown for example for the Brummer lipase (Grönke et al., 2005). In CG9186:eGFP overexpressing cells, however, the triacylglycerol content was not grossly affected as compared to that of untransfected cells or cells expressing only the GFP protein as determined by thin layer chromatography (Fig. 5D) or by a colorimetric assay (Fig. 5E). In order to test for the predicted lipolytic activity we assayed for trioleoylglycerol-, dioleoylglycerol-, and monooleoylglycerol hydrolase activity with artificial substrates (Fig. 5G). For this purpose, we overexpressed His-tagged CG9186 in COS-7 cells. Importantly, eYFP-tagged CG9186 targets to LDs and induces clusters in this heterologous cell system (Fig. 5F). As a positive control, we overexpressed the known lipolytic enzyme hormone-sensitive lipase (HSL) (Lass et al., 2006). HSL overexpression resulted in prominent enzymatic activity towards all three substrates when compared to *lacZ*-transfected cells (Fig. 5G). CG9186-expressing cell extracts, in contrast, showed activities comparable to that of the β-gal control (Fig. 5G). Expressing a mutant form of CG9186 predicted to lose any catalytic activity (serine 119 changed to alanine; CG9186S119A) also did not result in altered cellular lipid levels (Fig. 5D) or a changed lipolytic activity (data not shown). Taken together, these results indicate that CG9186 does not act as a neutral lipid hydrolase.

Intriguingly, however, the overexpression of CG9186S119A:eGFP causes a stronger LD clustering (Fig. 5B,C) than observed after expression of the CG9186:eGFP fusion protein (58% as compared to 51%) and a fusion of LDs (23%) which was rarely observed in wild type (0.15%) and only to a low degree (2.5%) in CG9186:eGFP-transfected cells. These results suggest that the

Fig. 1. CG9186 is an evolutionarily conserved LD-associated protein. (**A**) Phylogenetic tree of CG9186 and related sequences from different species. (**B**) Sequence alignment of CG9186 and homologous sequences of insects and mammals. Sequence identity in five or six species is shown in dark blue, identity in three or four species is shown in lighter shades of blue. The orange shaded boxes indicate the predicted catalytic center with the catalytic triad consisting of serine 119, aspartate 254 and histidine 283. (**C**) Schematic view of the CG9186 genomic locus, associated transcripts (turquoise) and resulting protein (blue), generated protein variants (yellow) and RNAi targeting sequences (black). (**D**) Homology-based model of CG9186. The model demonstrates accessibility of the protein targeting region (turquoise; amino acids 141–200) and the hypothetical arrangement of the annotated catalytic triad (black rectangle; the inset on the top left depicts an enlarged view). (**E**) Whole-mount *in situ* hybridization of *Drosophila* embryos using a CG9186 RNA antisense probe. CG9186 is maternally provided (embryonic stage 4) and later on (embryonic stages 12–13) is restricted to the salivary glands (asterisk). (**F**) Detection of CG9186 transcripts by *in situ* hybridization in combination with a fluorescent antibody staining for crebA, a marker for embryonic salivary glands (Fox et al., 2010). Embryos are oriented anterior to the left and dorsal side up.
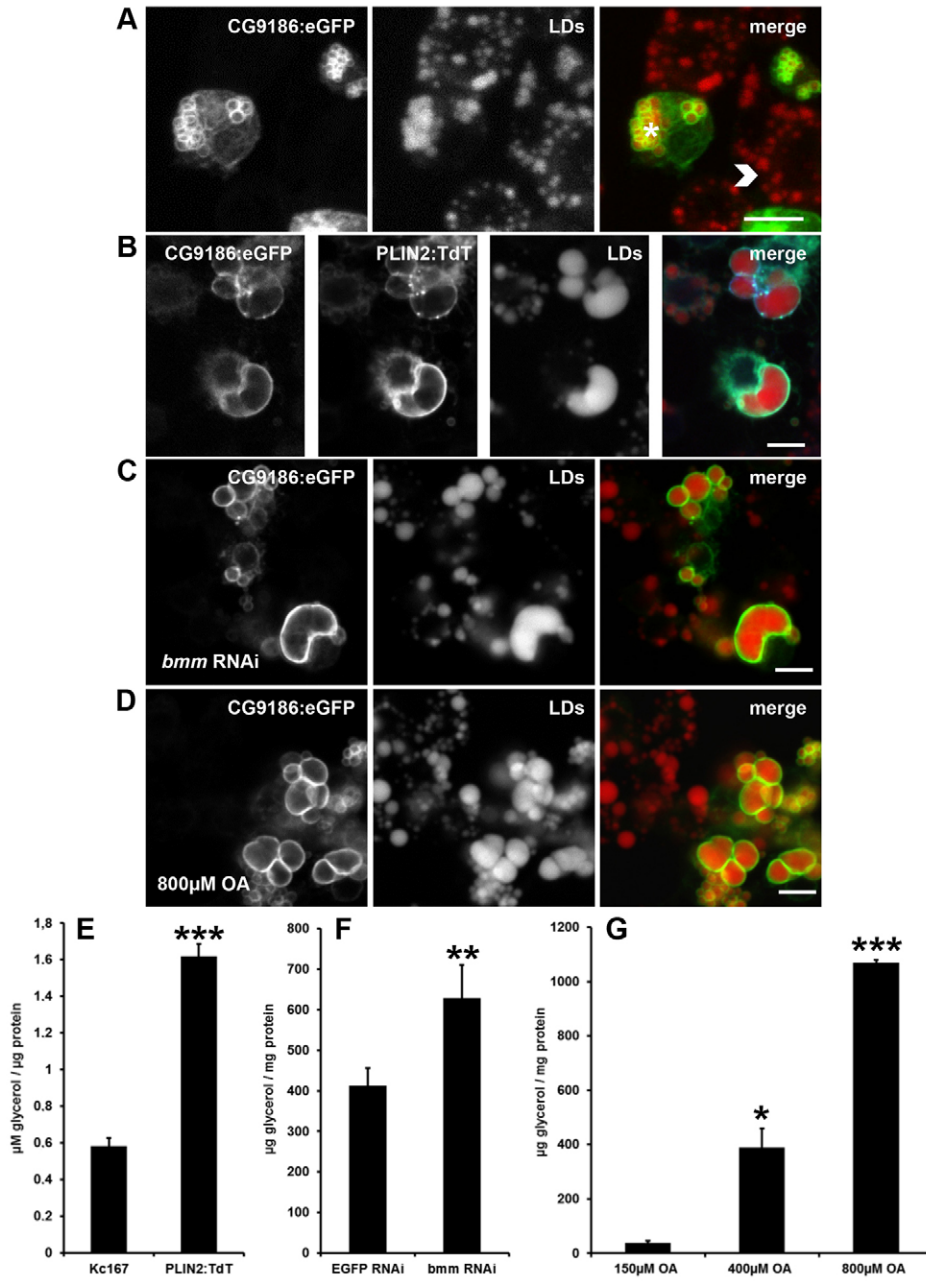
Fig. 2. Subcellular localization of CG9186:eGFP. (**A**) CG9186:eGFP localizes to LDs in *Drosophila* Kc167 cells and induces LD clusters (asterisk) whereas LDs of untransfected cells are dispersed (arrowhead). (**B**) Co-localization of CG9186:eGFP and PLIN2:TdT in Kc167 cells resulted in fused, irregular LDs, which are also seen following overexpression of CG9186:eGFP in cells treated with *brummer* RNAi (**C**) or 800 μM OA (**D**). (**E–G**) Quantification of the triacylglycerol increase induced by PLIN2:TdT overexpression, *brummer* RNAi or oleic acid loading. Acylglycerol levels in E were measured with the zenbio triglyceride measurement kit and in F and G with a colorimetric assay (Hildebrandt et al., 2011). Acylglycerol levels are normalized to total protein. Scale bars: 5 μm.

wild-type lipase-like domain of CG9186 formally counteracts the LD cluster induction caused by the CG9186 protein.

The CG9186-induced LD phenotype depends on a C-terminal clustering domain

In order to identify the sequences necessary for the CG9186 dependent LD clustering, we deleted various parts of the CG9186 protein (Fig. 1C) and assayed for the localization and function of the resulting protein variants in the absence (data not shown) or presence of 400 μM OA (Fig. 6A–E). Deletion of the N-terminal 140 amino acids [CG9186(Δ1–140):eGFP; Fig. 6A] or the C-terminal 106 amino acids [CG9186(Δ201–307):eGFP and CG9186S119A(Δ201–307):eGFP; Fig. 6B,C] of CG9186 had no effect on the association of the proteins with the LDs. However, deletion of the 106 C-terminal amino acids abrogated the LD-clustering phenotype as induced by

full length CG9186:eGFP overexpression [Fig. 6F; 62% of CG9186:eGFP-transfected cells harbored clustered LDs in comparison to 48% of CG9186(Δ1–140):eGFP and 10% of the CG9186(Δ201–307):eGFP-transfected cells]. Thus, the C-terminal part of the CG9186 protein is required for the LD cluster induction.

CG9186 contains a central LD association domain

In order to identify the sequence requirements of CG9186 for LD association, we continued our deletion analysis. When we extended the C-terminal truncation to amino acid 141 [CG9186(Δaa141–307):eGFP], the resulting protein accumulated in the cytoplasm (Fig. 6D). Conversely, an overexpressed GFP-tagged minimal protein spanning amino acids 141–200 of CG9186 targeted to LDs (Fig. 6E). Thus, this amino acid stretch is both necessary and sufficient for the LD association of CG9186.
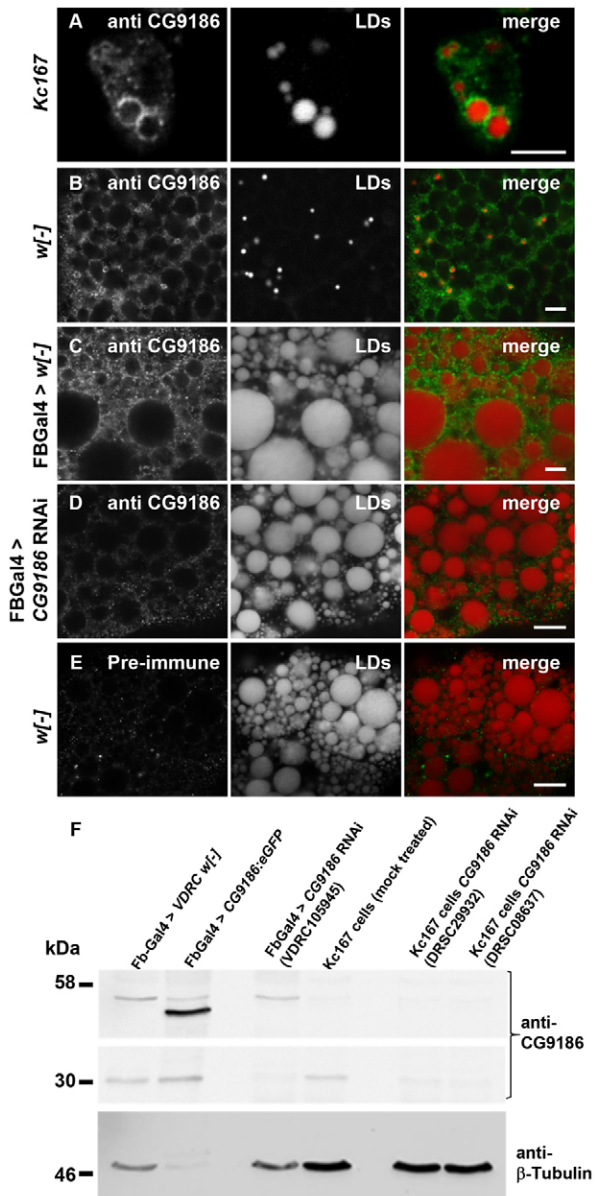
Fig. 3. Localization of endogenous CG9186 and specificity of the CG9186 antiserum. (**A–D**) Immunofluorescent stainings using the CG9186 antiserum, of (A) Kc167 tissue culture cells, (B) third instar larval salivary glands, (C) and third instar larval fat bodies of control animals (Fb-Gal4 driver with no activated transgene and (D) fat-body-enriched CG9186 RNAi transgene expression. (**E**) Fat body of *w[-]* control animals stained with the CG9186 pre-immune serum. LDs were counterstained with HCS LipidTOX. (**F**) Western blot of third instar larval fat body and tissue culture cell extracts. The fat body extracts were obtained from animals carrying a Gal4 activator driving fat-body-enriched expression (Fb-Gal4) of a CG9186:eGFP transgene, a CG9186 knockdown transgene (VDRC105945) or no transgene as a control (VDRC *w[-]*). The Kc167 cell extracts came from wild-type cells (mock treated), or cells targeted by two different dsRNAs reducing CG9186 transcript levels (RNAi treatment lasted six days). β-Tubulin served as a loading control. Scale bars: 5 μm.

Using our homology based modeling approach we predict that the 141–200 amino acid region of CG9186 (cyan protein part in Fig. 1D) is surface oriented and thus accessible for an interaction with the LD membrane. The analysis of this sequence with the NPS@ consensus secondary structure prediction server (Combet et al., 2000) in combination with Kyte and Doolittle plots (Kyte and Doolittle, 1982) identifies a possible alpha helix between positions 174 and 197 overlapping with a hydrophobic stretch between amino acids 174–200. Hydrophobic sequences, often in the form of amphipathic helices, are known to anchor proteins to LDs (Garcia et al., 2003; Hinson and Cresswell, 2009; Subramanian et al., 2004). Using a helical wheel plot of the CG9186 amino acids 179–197 we indeed found an enrichment of hydrophobic amino acids opposed by multiple hydrophilic and charged amino acids, suggesting an amphipathic character of the predicted helix (Fig. 6G). Thus, this hydrophobic stretch (aa 141–200) might represent the CG9186 anchoring sequence. This region of CG9186 is evolutionarily less well conserved as compared to most other parts of the protein, and thus it was important to ask whether also the CG9186 homologous sequences are able to associate with LDs.

Expression of the mouse homolog of CG9186 causes LD clustering

The murine homolog of CG9186 is an annotated gene termed MGI:1916082 (Fig. 1A,B). It encodes three protein isoforms with 35, 35 and 31% sequence identity to CG9186, respectively (amino acid homology: 52, 52 and 49%). We cloned the longest isoform of MGI:1916082, fused it to GFP, and expressed it in COS-7 cells. In the absence of lipid loading, the fusion protein co-localized with an ER marker protein as seen for CG9186 in fly cells (compare Fig. 7A and Fig. 4A). After induction of LD biogenesis by OA, the GFP-tagged MGI:1916082 translocated to the surface of LDs resulting in a LD-clustering phenotype as seen after CG9186 overexpression (compare Fig. 7A and Fig. 4B). Similar to the fly protein, MGI:1916082 lacked detectable neutral lipid lipase activity (supplementary material Fig. S1).

We next further characterized the possible cross species function of the two proteins. Similar to the expression of the fly CG9186 protein in COS-7 cells (Fig. 5F), heterologous expression of the murine MGI:1916082 protein in the fly Kc167 cells resulted in LD localization and clustering (Fig. 7B). Thus, not only the ability of the proteins to associate with LDs is evolutionarily conserved, but also to induce LD clusters.

In order to examine whether the expression pattern of MGI:1916082 is consistent with a fly corresponding function, we analyzed the transcript distribution of MGI:1916082 by northern blotting (Fig. 7C) and quantitative PCR (Fig. 7D) in different tissues of ad libitum fed and fasted mice, respectively. Fig. 7C,D show that MGI:1916082 is expressed in various lipid storing organs and tissues of mice, such as white and brown adipose tissue, the liver and muscles including the heart. No significant change of MGI:1916082 expression was seen between fed and fasted mice (Fig. 7C).

CG9186 regulates LD positioning and lipid stores *in vivo*

The prominent expression of CG9186 and MGI:1916082 in lipid storing tissues of both fly and mouse suggests a role of the proteins in organismic lipid storage regulation. As a test system to visualize possible cellular effects of altered CG9186 levels and activity, we used the salivary gland cells of *Drosophila* third instar larvae where the gene is prominently expressed (Fig. 3B). LDs in wild-type third instar larval salivary glands can be
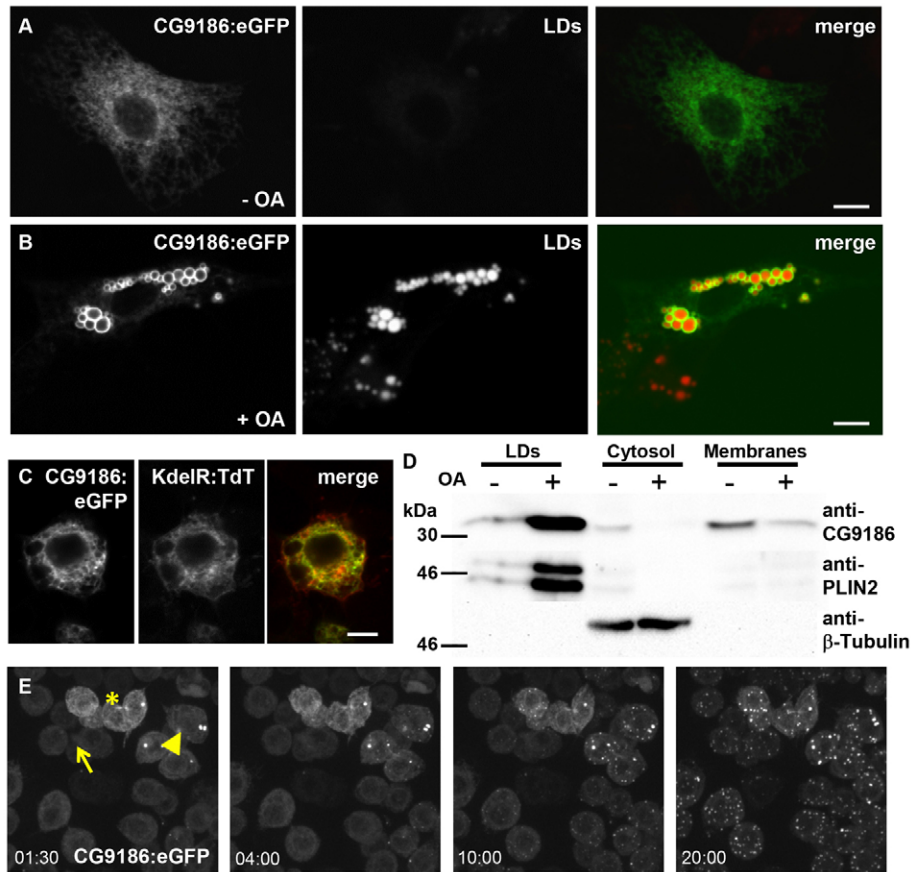
Fig. 4. CG9186 targets LDs via the ER. (**A**) In the absence of OA *Drosophila* ML-DmBG3-c2 cells show almost no LDs. Under these conditions CG9186:eGFP localizes in a reticular pattern reminiscent of the ER. (**B**) Upon addition of 400 µM OA, the ML-DmBG3-c2 cells deposit copious amounts of LDs decorated by CG9186:eGFP. (**C**) ML-DmBG3-c2 cells co-transfected with CG9186:eGFP and KdelR:TdT demonstrate ER localization of CG9186:eGFP. (**D**) Biochemical analysis of CG9186 subcellular localization. *Drosophila* Kc167 cells were grown in the absence or presence of OA. Cell extracts were prepared and the subcellular compartments were purified by subcellular fractionation. Equal volumes (20 µl of the LD fraction, 'LDs') or equal amounts of protein (10 µg of cytosolic or membrane proteins) of the respective fractions were subsequently probed in western blots with antisera detecting CG9186, PLIN2 or β-Tubulin. Please note that the cytosolic fractions contained much more total protein than the microsomal pellet. (**E**) Enlarged image frames from supplementary material Movie 1. The movie depicts the translocation of CG9186:eGFP from the ER to newly formed LDs. Kc167 cells stably transfected with CG9186:GFP were kept in low serum medium to avoid the deposition of LDs. At time point 0, OA-containing complete medium was added and every 10 seconds a z-stack of images were recorded with a spinning disc confocal system. Cells at 1 minute 30 seconds, 4 minutes, 10 minutes and 20 minutes post OA addition are shown. The cells of the polyclonal cell line differ in CG9186:eGFP expression level (arrow, arrowhead, asterisk). Cells that start with prominent CG9186:eGFP show LD-associated CG9186:eGFP by 10 minutes post OA addition (cells marked with asterisk or arrowhead). Cells lacking CG9186:eGFP expression need about 10 minutes longer until clear-cut localization can be seen (cells marked by arrow). Scale bars: 5 µm.

detected by the localization of the overexpressed bona fide LD-associated protein PLIN1 (Beller et al., 2010) as well as counterstaining with different neutral lipid staining dyes that mark LDs (Fig. 8A–D). Salivary gland LDs are numerous and dispersed throughout the cell (Fig. 8A–D). Thus, this tissue is an excellent test system to assay for a changed LD distribution. We first asked whether the LD-clustering phenotype in response to overexpression of the wild-type CG9186 and the mutant CG9186S119A protein is also observed when corresponding transgenes are expressed in the salivary glands using the Gal4/UAS expression system (Brand and Perrimon, 1993). We used Gal4 activators showing either expression in the fat body and salivary glands (Fb–Gal4) or salivary glands only (Sgs3–Gal4). Fig. 8E shows that overexpression of CG9186:eGFP in salivary gland cells resulted in clustered LDs as had been seen in the Kc167 and mammalian cell systems. As seen in the fly tissue

culture cells, the LD-clustering phenotype was enhanced when the CG9186S119A:eGFP point mutation was overexpressed (Fig. 8F). These results indicate that the overexpression of CG9186 affects the LD distribution *in vivo* as had been observed in the tissue culture cells.

In order to investigate if reduced CG9186 protein levels would also result in an LD phenotype, we targeted CG9186 encoding transcripts by transgene-derived RNAi. Knockdown efficacy was confirmed by western blotting and antibody staining (Fig. 3C–F). We assayed first for an effect on the salivary gland LDs. Transgene-derived CG9186 RNAi was expressed using the Gal4/UAS system (Brand and Perrimon, 1993) with a Gal4 activator line driving expression in fat bodies and salivary glands (Fb-Gal4), salivary glands enriched (Sgs3-Gal4) or ubiquitous expression (Tubulin-Gal4). In all cases, the reduction of CG9186 protein in wandering *Drosophila* third instar larval
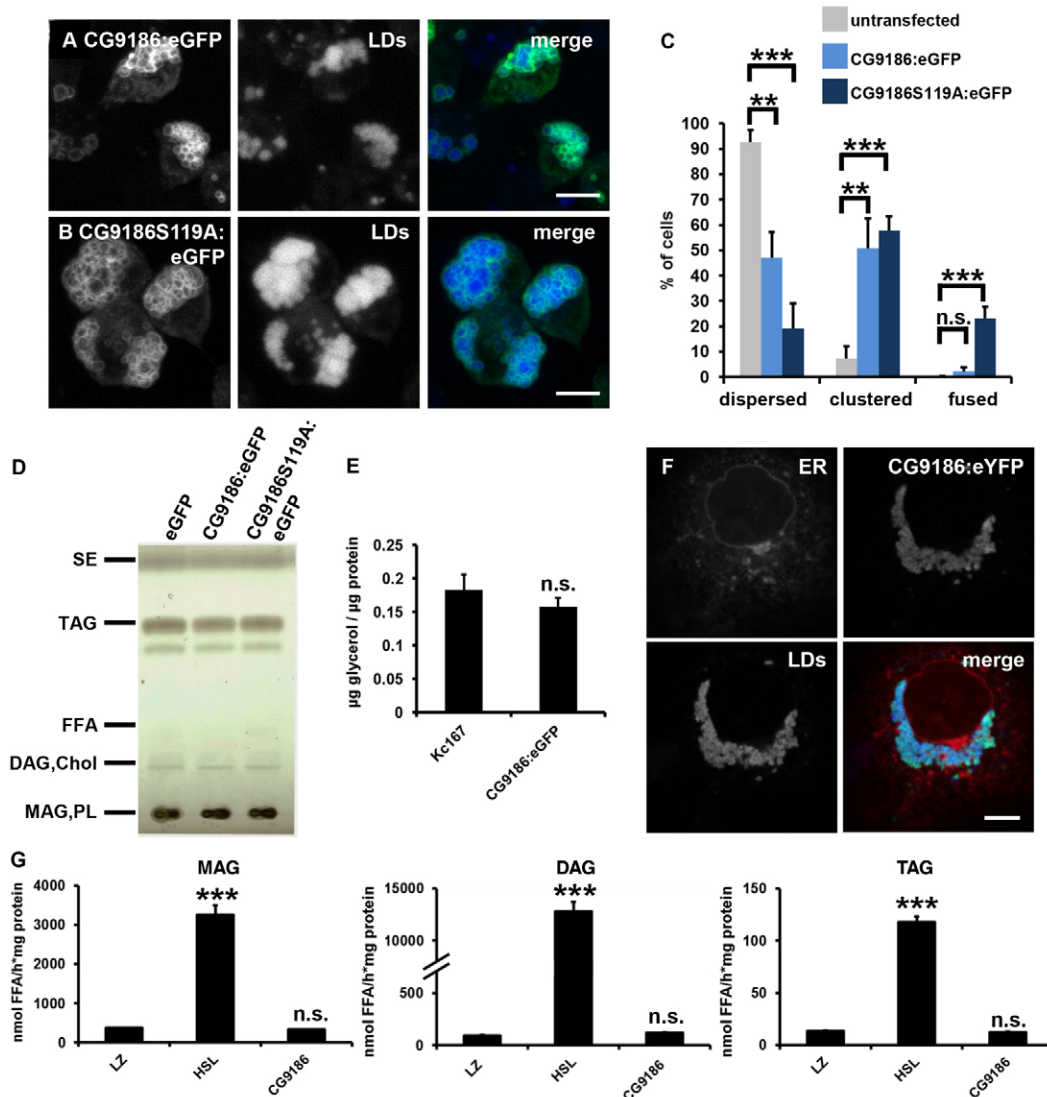
Fig. 5. **CG9186 regulates LD positioning and is not involved in lipid remobilization.** (**A**,**B**) Maximum intensity projections of z-stacks of *Drosophila* Kc167 cells expressing CG9186:eGFP (A) and CG9186S119A:eGFP (B) 40 hours post transfection. LDs were induced with 400 μM OA. (**C**) Cells as shown in A and B, as well as neighboring untransfected cells, were analyzed for their respective LD phenotype. Bars represent the averaged results from three biologically independent experiments. In total, the LD patterns of 638 untransfected cells, 699 CG9186:eGFP-transfected and 650 CG9186S119A:eGFP-transfected cells were visually analyzed. Error bars indicate s.d. (**D**) The lipid content of cells stably expressing eGFP, CG9186:eGFP or CG9186S119A:eGFP was analyzed by thin layer chromatography. (**E**) Acylglycerol content of wild-type Kc167 cells and cells stably expressing CG9186 was analyzed with a colorimetric assay (Hildebrandt et al., 2011). LDs were induced overnight with 400 μM OA. (**F**) eYFP-tagged CG9186 protein targets LDs in COS-7 cells and induces LD clustering. (**G**) Lipolytic activity towards trioleoylglycerol (TAG), dioleoylglycerol (DAG) or monooleoylglycerol (MAG) of COS-7 cells transiently transfected with constructs expressing β-Gal (LZ), hormone sensitive lipase (HSL) or CG9186. Scale bars: 5 μm (A,B) and 10 μm (F).

salivary gland cells resulted in a nearly complete depletion of LDs (Fig. 8G; data not shown), indicating that CG9186 activity is necessary for the proper formation of LDs in salivary glands. As a consequence, the fat storage of those cells is expected to also be reduced.

We finally asked whether a corresponding reduction of CG9186 activity causes reduction of the fat storage in the whole organism. For this we utilized the Gal4/UAS system (Brand and Perrimon, 1993) to express CG9186 RNAi under control of the ubiquitous Tubulin–Gal4 (data not shown) or Actin–Gal4 (Fig. 8H) activator, which both result in a global knockdown of the protein. Then, we examined the fat stores of

6-day-old male flies expressing the RNAi transgene or lacking the transgene (control flies). Fig. 8H shows that the CG9186 RNAi expression results in a reduction of the triacylglycerol content of the flies to about 60% of the content in control flies. Thus, CG9186 is not only necessary for proper LD distribution but also for adequate fat storage capabilities in flies.

Discussion

This study provides evidence that the evolutionarily conserved protein CG9186, which was previously found in LD preparations of *Drosophila* embryos (Cermelli et al., 2006) and third instar larval fat bodies (Beller et al., 2006), is a member of a novel
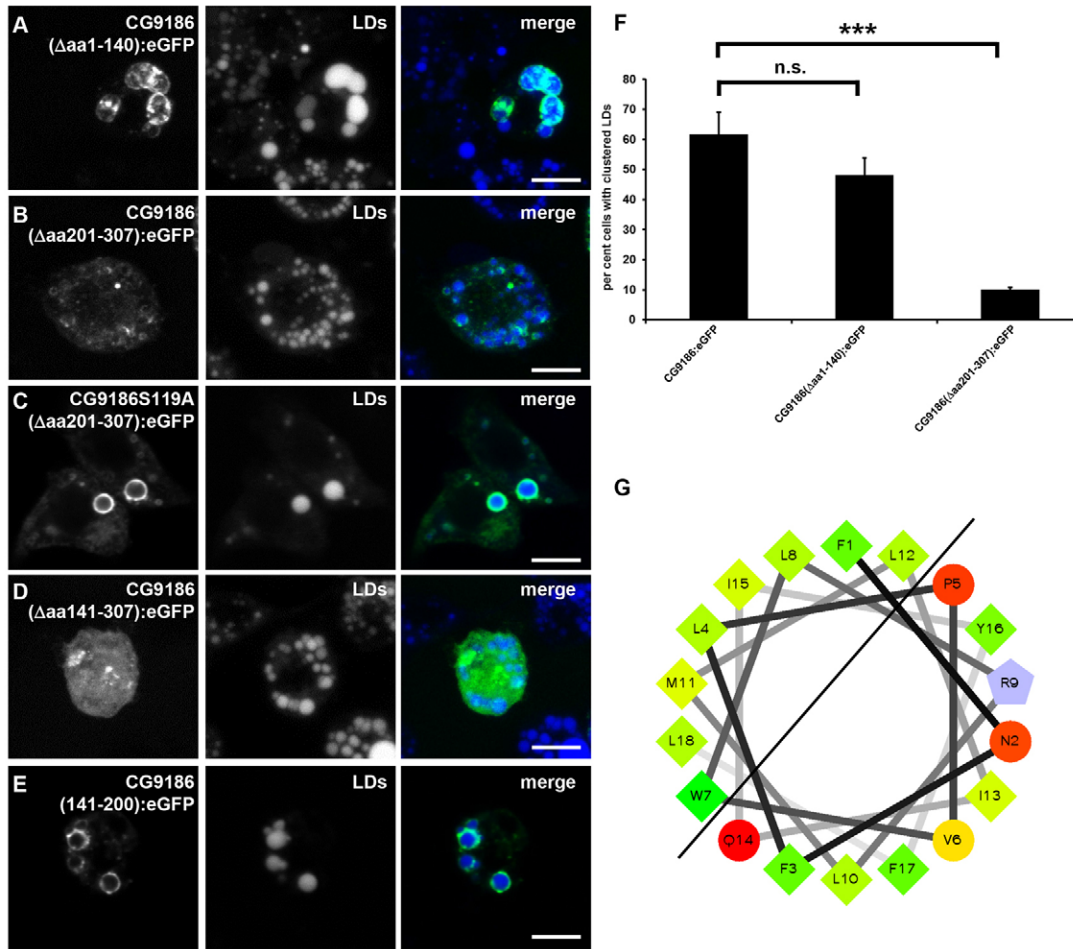
Fig. 6. Structure–function analysis of CG9186. (A–E) eGFP-tagged CG9186 deletion constructs expressed in *Drosophila* Kc167 cells in the presence of 400 μM OA. (**F**) Cells expressing CG9186:eGFP (174 cells), CG9186(Δ1–140):eGFP (121 cells) or CG9186(Δ201–307):eGFP (151 cells) were analyzed visually for the LD-clustering phenotype. Bars represent the mean of three separate experiments. Error bars indicate s.d. (**G**) Helical wheel plot of amino acids 179–196 (FNFLPVWLRLMLIQIYFL′) of CG9186. Hydrophilic residues are shown as circles, hydrophobic residues as diamonds and potentially positively charged residues as pentagons. Hydrophobicity is represented by green shading (darker green is more hydrophobic) and hydrophilicity by red colouring. Potentially charged residues are shown in blue. The line indicates the border between hydrophobic and hydrophilic residues. Scale bars: 5 μm.

LD-associated protein family. CG9186 as well as its mouse homolog MGI:1916082 are involved in lipid droplet regulation, since overexpression affects the distribution of LDs within cells. In addition, experimentally induced CG9186 level modulations in flies have the same effects on LDs and affect the fat storage of the organism.

As observed with a number of LD-associated proteins, CG9186 shows a dual localization pattern in cells. Both, results from biochemical fractionation studies and visual inspection by time-lapse microscopy experiments show that in the absence of LDs CG9186 is associated with the ER and that upon OA stimulated LD formation, it associates with the increasing number of LDs. The protein domain which is both necessary and sufficient for ER/LD association maps to an internal region of 60 amino acid residues which, however, lacks a known ER targeting signature, such as a KDEL sequence or sequences described for tail-anchored proteins (Borgese and Fasana, 2011). So far, we could not identify CG9186 fragments targeting to only one of the two locations. Thus, it appears very likely that the region required for ER association of the protein is identical with

the one required for LD association. Both, the translocation of CG9186 from the ER to LDs and the finding of a protein region that is needed for ER and LD association of the protein is consistent with the current model of LD biogenesis, proposing that LDs derive through a budding process from the ER (Farese and Walther, 2009). Since we have not performed replacement studies with individual amino acid residues of the ER/LD association domain, we cannot exclude the possibility that the distinction between ER and LD targeting rests on distinct amino acid residues or a combination of them. Additional experiments will be needed to identify the residues and mechanisms underlying ER targeting by this novel family of proteins which undergo ER/LD translocation such as CG9186.

Expression of CG9186 and its murine homolog in both homologous and heterologous tissue culture cells demonstrate that their ER/LD targeting features are evolutionarily conserved, although the sequence similarity within the ER/LD association domain is rather low. We therefore suspect that LD localization rather depends on structural features as opposed to a distinct amino acid motif. Given the wide array of different LD
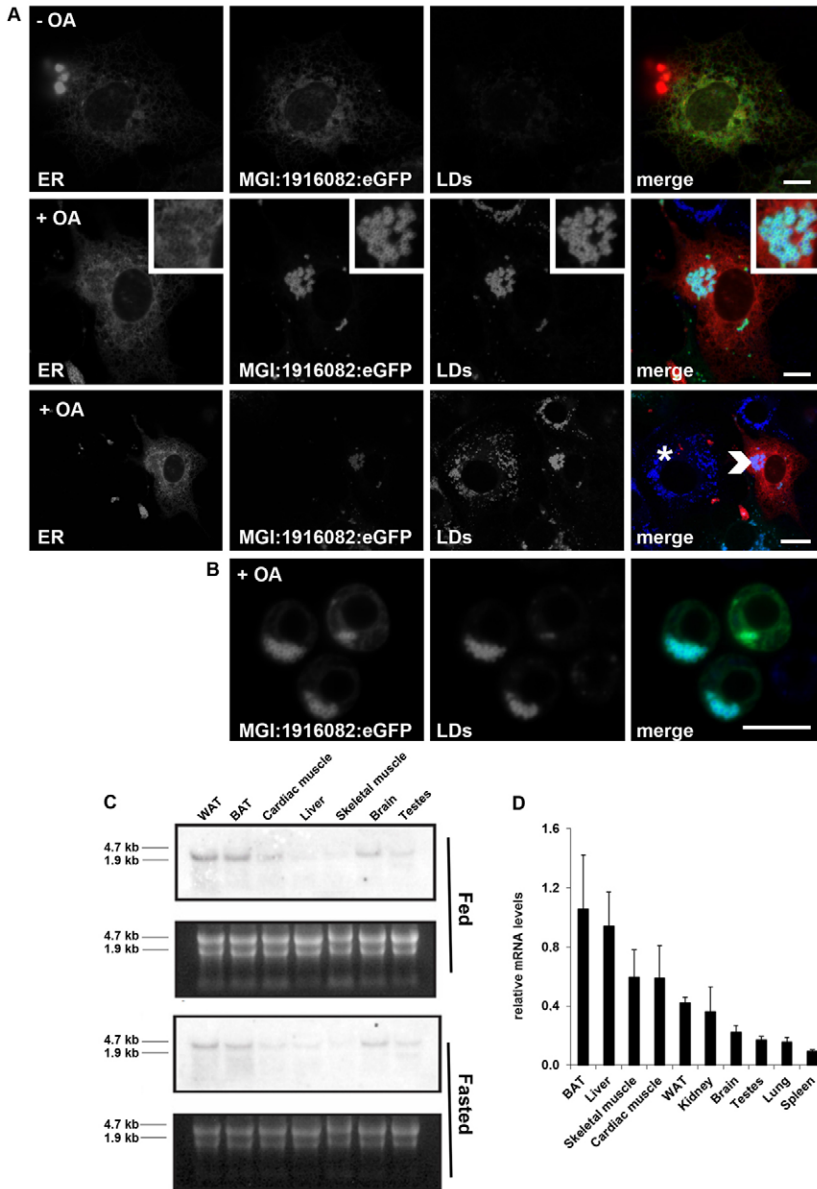
Fig. 7. CG9186 function is evolutionarily conserved.
(**A**) Expression of an eGFP-tagged fusion protein of the murine CG9186 ortholog MGI:1916082 in COS-7 cells. In the absence of lipid loading the protein localized at the ER. Upon incubation with OA MGI:1916082 translocated to LDs. The images in the third row show a wider field of view of cells expressing MGI:1916082:eGFP (arrowhead) next to untransfected cells (asterisk) reveal that LDs are dispersed in non-expressing cells in contrast to the clustered LDs in the transfected cells. (**B**) Expression of GFP-tagged MGI:1916082 in *Drosophila* Kc167 cells results in LD targeting and clustering. (**C**) Northern blot analysis of the expression of MGI:1916082 encoding transcripts in various tissues. (**D**) qRT-PCR of the different tissue samples. Relative expression levels normalized to MGI:1916082 expression in brown adipose tissue (BAT) and β-Actin as a reference gene. WAT, white adipose tissue. Scale bars: 10 μm.

localization sequences that have been identified so far and the fact that they lack an obvious consensus sequence, a distinct sequence based LD association motif is unlikely. This conclusion is supported by the fact that mammalian LD-associated PERILIPIN proteins are targeted even to LDs of bacteria when expressed in the prokaryotic cells (Hänisch et al., 2006). In case there would be a sequence-based targeting mechanism, which rests on distinct sequence-dependent interactions with components of a targeting machinery, corresponding factors of such machinery should be functionally conserved between eukaryotes and bacteria. However, given the evolutionary distance and the different modes of LD formation, such a scenario appears unlikely. Thus, the available evidence is more consistent with the proposal that the association of CG9186 with the ER is based on the structure of the targeting sequence and that the subsequent localization of the protein with LDs is a consequence of the biogenesis of LDs, i.e. their origin from ER.

Overexpression of CG9186 or its mammalian homolog MGI:1916082 in OA-induced *Drosophila* and mammalian tissue culture cells caused clustering of LDs (e.g. Fig. 5A–C,F; Fig. 7A,B). This phenotype was also obtained after transgene-derived overexpression of CG9186 in salivary glands of *Drosophila* larvae, where in comparison with the cells of the canonical fat storage tissue, the density of LDs is low enough to visualize the clustering phenotype (Fig. 8E,F). LD cluster induction is not expected for a functional lipase involved in the mobilization of lipids. Instead, one would expect that lipase overexpression causes a mobilization of the lipid stores as recently shown for the Brummer lipase (Grönke et al., 2005). Lack of lipase activity of CG9186 is further supported by the finding that CG9186 failed to exert neutral lipid lipase activity in cell extracts (Fig. 5G; data not shown). Although our studies do not rule out that CG9186 exerts a specific or very weak lipolytic activity, its function as a canonical neutral lipid lipase similar to Brummer can be excluded. Despite the fact that CG9186
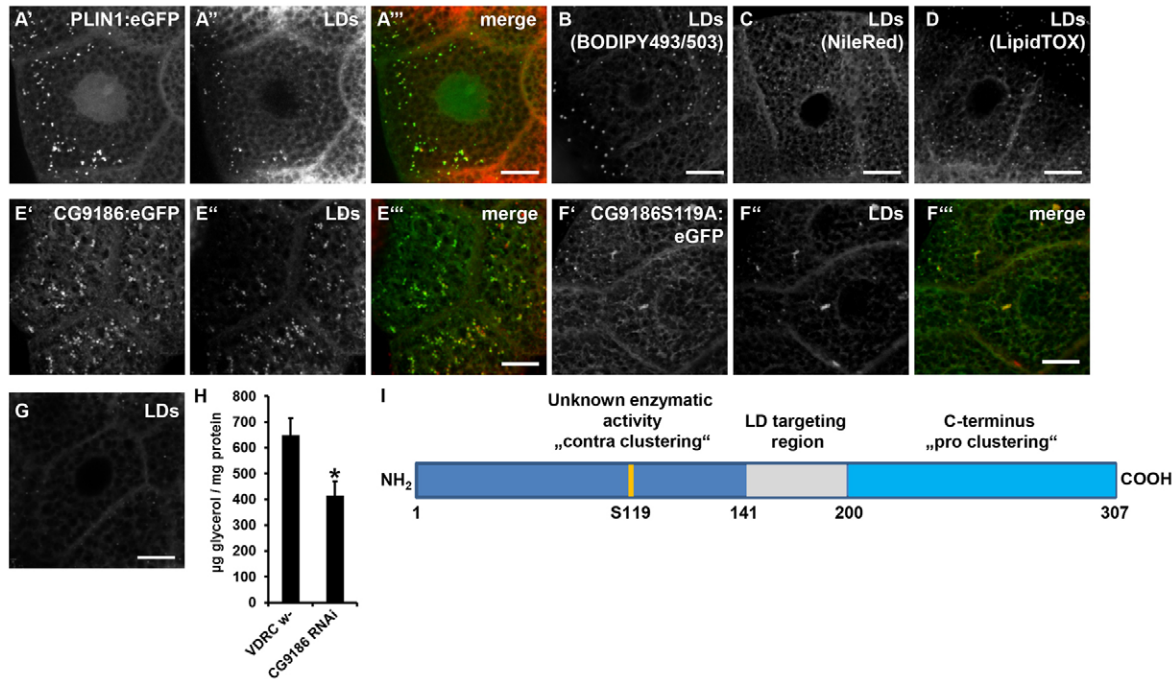
Fig. 8. CG9186 is involved in organismic lipid storage regulation. (A–D) Salivary glands of *Drosophila* third instar larvae store dispersed LDs as shown by: (A) localization of the *bona fide* LD-associated protein PLIN1:eGFP (Beller et al., 2010) to LipidTOX-positive spherical particles; (B–D) different neutral lipid stains. **(E)** Transgene-derived CG9186:eGFP overexpression results in a clustering of LDs in third instar larval salivary glands. **(F)** This clustering phenotype is enhanced when the mutated CG9186S119A:eGFP protein is overexpressed. **(G)** Ubiquitous or salivary gland enriched RNAi-mediated targeting of CG9186-encoding transcripts results in a reduction of salivary gland LDs. A–G are maximum intensity projections of z-stacks. **(H)** Ubiquitous RNAi-mediated knockdown of CG9186 results in decreased overall TAG storage levels in 6-day-old flies, fed *ad libitum*, compared with control flies lacking the transgene (VDRC *w[-]*). **(I)** Functional domains of CG9186 identified in the present study. Schematic drawing of the CG9186 sequence depicting important protein regions with the respective functional information uncovered by our studies. Scale bars: 20 μm.

possesses the diagnostic sequence motif for the catalytic site of lipases, the protein could also act, for example, as an acyltransferase or a phospholipid modifying enzyme, a speculation that will be addressed in future biochemical studies.

LD clustering and LD size changes have recently been shown to be caused by activity changes of certain proteins involved in LD homeostasis. These proteins include Fsp27/Cidec (Jambunathan et al., 2011), Cidea (Christianson et al., 2010), Fld1p/Seipin (Fei et al., 2011b), Atg2A and B (Velikkakath et al., 2012), and the Hepatitis C Virus core protein (Depla et al., 2010). While Cidec, Cidea and the Hepatitis C Virus core protein induce LD cluster formation upon overexpression (Christianson et al., 2010; Depla et al., 2010; Jambunathan et al., 2011) as shown here for CG9186 and MGI:1916082, LD clusters are also formed in response to the reduced activity of proteins, such as Fld1p/Seipin and Atg2A and B, caused by mutations or RNAi knockdown (Fei et al., 2008; Szymanski et al., 2007; Velikkakath et al., 2012). Thus, LD cluster formation is not caused by simply overexpressing LD-associated proteins. Instead, it represents a distinct cellular phenotype which is typical for activity changes of a subset of LD-associated and LD-regulatory factors. This conclusion is also supported by the fact that the majority of the recently identified LD-associated proteins (Beller et al., 2006) that were overexpressed under the same conditions as used here for CG9186, had no effect on LD positioning (data not shown).

Recent results have shown that LD positioning and LD size regulation can be affected by changing the phosphatidic acid

(PA) and phosphatidylcholine (PC) levels of the LD hemimembrane (Fei et al., 2011a; Krahmer et al., 2011). Increased levels of PA results in LD fusion, whereas increased levels of PC appear to act as an 'anti-fusogen' (Fei et al., 2011a; Yang et al., 2012). Thus, mutations or reduced activity levels of PC synthesis pathway components cause LD clusters and coalesced giant LDs (Guo et al., 2008; Krahmer et al., 2011). Indeed, at least some of the aforementioned protein-induced LD cluster and size effects are caused by an altered phospholipid composition of the LD membrane. For example, LD clustering following Fld1p/Seipin inactivation appears to be based on altered phosphatidic acid levels (Fei et al., 2011a). Based on these findings, it seems reasonable to speculate that CG9186/MGI:1916082 overexpression also affects the surface properties of LDs either directly by a yet unknown phospholipid modifying enzymatic activity or more indirectly via protein–protein interactions with corresponding regulatory components. The structure–function and mutation analyses reported in this study revealed that the C-terminus of CG9186 is necessary to induce LD clusters (Fig. 6B,C,F). Furthermore, a point mutation of serine 119 appears to counter-balance LD cluster induction, since a serine to alanine exchange results in an increased propensity to induce LD clusters in tissue culture and salivary gland cells (Fig. 5A–C; Fig. 8E,F). Thus, we identified two separate features within the CG9186 protein (Fig. 8I), affecting LD positioning and potentially LD architecture.

CG9186 overexpressing cells additionally seem to have difficulties to package excessive amounts of lipids properly

since we noted in many overexpressing cells fused LDs when elevated lipid storage levels were present (Fig. 2). Similarly, fused LDs were present when the mutant CG9186S119A protein variant was expressed (Fig. 5A–C). We expect that the fused LD phenotype is directly or indirectly the result of the LD clustering. The data are thus in agreement with a model in which proper CG9186 levels are needed to facilitate efficient lipid packaging or LD biogenesis control.

Expression of CG9186 as well as its mammalian homolog MGI:1916082 is highly enriched in lipid storing tissues such as the fat body of the fly and the white and brown adipose tissue of mice (Chintapalli et al., 2007) (Fig. 7C,D). In addition, we found strong CG9186 expression during all ontogenetic stages in the *Drosophila* salivary gland cells. Interference with CG9186 expression levels by either CG9186 RNAi knockdown or overexpression in salivary glands had a strong impact on the amount of stored lipids and LD positioning (Fig. 8A–G). This finding is surprising, since the function of LD deposits in salivary glands is not clear. It was recently reported that LDs are absent from fly salivary glands under normal growth conditions (Tian et al., 2011). In contrast, we and others (Yu et al., 2011) microscopically observed copious LDs in larval salivary glands, which also show a prominent triacylglycerol accumulation in lipidomics analyses (Carvalho et al., 2012). Similarly, salivary gland lipid deposits were reported from other *Drosophila* species (Harrod and Kastritsis, 1972). A possible function of salivary gland LDs could be linked to the most prominent function of this tissue, which is the production and secretion of glue proteins used to attach the pupa to the substrate (Beckendorf and Kafatos, 1976; Fraenkel and Brookes, 1953). However, animals that overexpress CG9186 or contain reduced levels of CG9186 due to RNAi knockdown had no problems to properly attach as pupae. Thus, we speculate that the stored lipids in salivary glands might serve other functions which are yet to be identified.

In addition to the tissue specific phenotype of CG9186 RNAi knockdown, ubiquitous targeting of CG9186 encoding transcripts results in decreased overall storage lipid levels (Fig. 8H). CG9186, however, does not appear to be essential for LD biogenesis. This notion is based on our findings that we still see prominent amounts of LDs in tissue culture cells (supplementary material Fig. S2) and fat bodies of third instar larvae (e.g. Fig. 3D) following CG9186 RNAi knockdown. While the RNAi treatment itself appears efficient as shown by the reduction of CG9186 protein levels below the detection limit of our antibodies (Fig. 3D,F), we currently do not rule out that the CG9186 RNAi knockdown leaves residual gene activity and that the phenotype of a CG9186 null mutation would be more severe.

The results presented in this study describe two members of a novel LD-associated protein family, CG9186 and its mammalian homolog MGI:1916082, which regulate the subcellular positioning of LDs and affect the lipid storage levels of the organism. The two proteins are initially associated with the ER and subsequently with LDs. This finding not only supports the argument that LDs derive from the ER, but also delivers a tool to visualize and study LD biogenesis in detail. Our results further imply that altering CG9186 or MGI:1916082 activities interferes with the distribution of LDs within the cell as well as the packaging of fat into these lipid storage organelles. It is fully conceivable that each one of these processes alone or the combination of both contributes to the reduced fat storage capability of individuals that contain strongly reduced CG9186 levels. The results also establish the salivary glands of flies as an experimental system in which questions concerning the biogenesis of LDs and the regulatory mechanism underlying energy storage of cells can be addressed.

Materials and Methods
Molecular biology and cloning
The CG9186 open reading frame was PCR-amplified from the EST clone LP01162 (*Drosophila* genomics resources center; DGRC) with the *Not*I containing forward (5′-gcttgcggccgccaccATGCAGGAGGCCTACGTCAACATCAAC-3′) and *Asc*I containing reverse (5′-gcaaggcgcgccTCAAACACGTCTGTGCTGCTGGATC-3′) primer pair. The amplicon was directionally cloned in the pENTR/D-TOPO vector (Invitrogen), which was subsequently used for Gateway-recombination-based (Invitrogen) transfer of the gene into destination vectors for tissue culture expression of GFP fusion proteins (pUbiP-EGFP-rfa, gift from A. Herzig) or germline transformation vectors for expression of GFP-tagged fusion proteins using the Gal4/UAS system (pTGW, DGRC). Deletion constructs were engineered by PCR-mediated site directed mutagenesis (primer sequences available upon request).

The KdelR-encoding sequence was PCR-amplified from the EST clone LD06574 (DGRC) with the *Not*I containing forward (5′-gcttgcggccgccacc-ATGAATATCTTTCGCTTTGCTGGGG-3′) and *Asc*I containing reverse (5′-gcaaggcgcgccCTGCCGGCAGCTGGAGCTTCTTGC-3′) primer pair. The other cloning steps were identical to the cloning of CG9186, however, a different tissue culture expression vector was used (C-terminal fusion of TdT; pUbiP-rfA-TdT, gift from A. Herzig).

The coding sequence of murine MGI:1916082 was amplified by PCR using white adipose tissue cDNA as template. MGI:1916082 forward primer, 5′-GTGGAATTCGCCTCAGAAGTCGAGGAACAAATC-3′, and MGI:1916082 reverse primer, 5′-AGACTCGAGCTATTTTCTGGGCGGTCTATTATTTATC-C-3′, were designed according to GenBank™ entry NM_172401. The Amplicon was cloned into the pcDNA4/Hismax C vector (Invitrogen) using the *Eco*RI and *Xho*I restriction sites. For subcloning into pEGFP-C1 and pEYFP-C1 vectors (Clontech), the coding sequences were re-amplified by PCR using the forward primer 5′-AGATCTCGAGCTATGGCCTCAGAAGTCGAGGAAC-3′, and the reverse primer 5′-GCTTCGAATTCTCTATTTTCTGGGCGGTCTATTATTTA-TCC-3′ for MGI:1916082, as well as the forward primer 5′-GCACTCGAGC-TCAGGAGGCCTACGTCAACA-3′ and the reverse primer 5′-GACGAATTC-TCAAACACGTCTGTGCTGC-3′ for CG9186. The PCR products were ligated into the vectors using the *Eco*RI and *Xho*I restriction sites.

CG9186 targeting dsRNAs were synthesized using the Megascript T7 *in vitro* transcription kit (Ambion) according to the manufacturer's instructions using PCR-derived templates based on gene-specific primers pre-computed by the Harvard RNAi screening center (www.flyrnai.org).

Antibody production
Custom antibodies detecting CG9186 were obtained from Peptide Speciality Laboratories (www.peptid.de). Two rats were immunized each with peptides comprising amino acids 67–86 (AGHDDPPEASIREVPQLSGN) and 262–280 (YDQLKKDYPKVDAQLDTKK) of CG9186. We selected the serum with the better reactivity on the basis of western blot and immunofluorescence tests.

Tissue culture, transfections and RNA interference
Drosophila Kc167 (Harvard RNAi screening center) and ML-DmBG3-c2 (DGRC) cells were cultured in Schneider's medium (Invitrogen) including Penicillin/Streptomycin (Invitrogen) and 10% heat inactivated fetal calf serum (PAA) following standard procedures [ML-DmBG3-c2 cell medium was additionally supplemented with 10 µg/ml insulin (Sigma)]. Effectene (Qiagen) or Fugene (Promega) were used as transfection reagents according to the manufacturer's instructions. Stable transfected Kc167 cells expressing PLIN2:TdT, CG9186:eGFP or CG9186S119A:eGFP were obtained by co-transfection with the pCoBlast (Invitrogen) resistance plasmid and selection with 10 µg/ml Blasticidin. LDs were induced with 400 or 800 µM oleic acid (Calbiochem) complexed to 0.4% fatty-acid-free BSA (Sigma). RNA interference with the bathing protocol was performed as described previously (Beller et al., 2008).

COS-7 cells were maintained in DMEM containing 10% FCS, 100 units/ml Penicillin, and 100 µg/ml Streptomycin at 37℃ in humidified air (95%) and 5% CO$_2$. For transfection, cells were seeded in 100 mm dishes at a density of ~900,000 cells/dish or in 8-well-chamber slides (Sarstedt) at a density of ~10,000 cells/well. Approximately 12 hours after seeding, cells were transfected using Fugene (Promega) or Metafectene (Biontex) as transfection reagents according to the manufacturers' instructions.

Gene expression analysis by RNA *in situ* hybridization, quantitative PCR and northern blot analysis
RNA *in situ* hybridization
RNA *in situ* hybridizations with an antisense probe based on the CG9186 EST clone LP01162 (DGRC) were performed as described previously (Grönke et al.,

2003) with colorimetric detection and as described previously (Beller et al., 2010) with fluorescent detection. Instead of the Vectastain ABC reagent, however, we used peroxidase conjugated streptavidin. Colorimetrically stained embryos were dehydrated and embedded in Canada balsam (Sigma-Aldrich) and subsequently images were recorded with a Zeiss Axiophot upright microscope with a Kontron camera and a 20× air objective. The fluorescently stained embryos were counterstained with an anti-crebA antiserum (DSHB; dil. 1:5,000) detected by an anti-rabbit Dylight598 conjugate. Embryos were embedded in 50% PBS/Mowiol and imaged with a Zeiss LSM780 confocal microscope.

Northern blot analysis

Northern blot analysis was performed as previously described (Kienesberger et al., 2008). In brief, adult male C57BL/6 mice between 12 and 16 weeks of age were maintained on a regular light:dark cycle (14 hours light, 10 hours dark) and fed a standard laboratory chow diet (4.5% wt/wt fat). Tissue samples were collected from fed (*ad libitum* access to food and water overnight) or fasted (food was removed for 16 hours) animals between 09:00 and 10:00 hours. Total RNA was extracted and probed in northern blots using [α-^{32}P]dATP (Amersham Biosciences)-labeled DNA probes corresponding to bp 4–684 of the MGI:1916082 coding sequence. Radioactivity was visualized by exposing the membrane to a ^{32}P-imaging screen (Amersham Biosciences) and scanning with a PhosphorImager (Storm 860, Amersham Biosciences).

Real-time PCR

Real-time PCR analysis of MGI:1916082 was performed as described previously (Taschler et al., 2011) using the forward primer 5′-GGTCTGAATGGTCAAATA-GAGCA-3′ and the reverse primer 5′-GTCATATAGGTGCCTACGGAATG-3′. Relative mRNA levels were calculated using the $\Delta\Delta C_T$ method and β-Actin as reference gene.

Microscopy and immunohistochemistry

Transfected cells were either fixed with 5% paraformaldehyde and permeabilized with 0.1% Triton X-100 before they were counterstained with a LD dye and embedded in Mowiol (Fig. 2A–D; Fig. 4A–C; Fig. 5A,B; Fig. 6A–E; supplementary material Fig. S1), or imaged via live microscopy in chamber slides filled with medium containing LD dye (Fig. 4E; Fig. 5F; Fig. 7A,B). Salivary glands were imaged live in 30% glycerol in PBS (Fig. 8A–G).

Antibody stainings were performed as described previously (Beller et al., 2010). In brief, cells and tissues (Fig. 3A–E) were fixed with 5% paraformaldehyde, permeabilized with 0.1% Triton X-100 and incubated with anti CG9186 (dil. 1:2,000) or the pre-immune serum in the same dilution. Secondary antibodies were conjugated with Alexa Fluor 568 (Molecular Probes). LDs were counterstained with either Nile Red (10 mg/ml in DMSO; 1:40,000; Molecular Probes), BODIPY 493/503 (10 mg/ml in ethanol; 1:2,000; Molecular Probes) or HCS LipidTOX deep red (1:250–1:1,000; Molecular Probes). Images were recorded with a Leica TCS SP2 AOBS, a Leica TCS SP5 or a Zeiss LSM780 microscope. Time-lapse movies were recorded with an Olympus-based Ultraview VOX (Perkin Elmer) imaging system.

Storage lipid quantification

Storage lipids were quantified with an enzyme-coupled colorimetric reaction as described previously (Hildebrandt et al., 2011). Triglyceride quantification depicted in Fig. 2E was performed with the Zenbio Triglyceride assay kit (www.zen-bio.com) according to the manufacturer's instructions.

Thin layer chromatography was performed essentially as described previously (Taschler et al., 2011) with the alteration that the lipids were extracted by a chloroform/methanol mixture from cells grown in six-well plates.

Fly husbandry and crossings

Flies were kept on a complex cornflour–soyflour–molasses food, supplemented with dry yeast in a 12 hour:12 hour light:dark cycle at 25℃ and 20–30% humidity. Fly stocks used were: UAS-CG9186:eGFP (this study); UAS-CG9186S119A:eGFP (this study); UAS-CG9186 RNAi [VDRC105945 (Dietzl et al., 2007)]; *white[-]* [VDRC60000; (Dietzl et al., 2007)]; Fb-Gal4 (Grönke et al., 2003); Actin-Gal4 (Bl4414, Bloomington Stock Center); Tubulin-Gal4 (gift from A. Herzig) and Sgs3-Gal4 (Bl6870, Bloomington Stock Center).

Subcellular fractionations and western blotting

Subcellular fractionations of *Drosophila* Kc167 tissue culture cells were performed essentially as described previously (Beller et al., 2006). In brief, confluent *Drosophila* Kc167 cells in 75 cm^2 flasks were grown for 15 hours in the presence of 5 μg/ml cycloheximide either in standard medium or medium supplemented with 400 μM OA. Cells were subsequently collected in 1 ml FBB (10 mM HEPES pH 7.6, 10 mM KCl, 0.1 mM EDTA, 0.1 mM EGTA, 1 mM DTT, Roche EDTA-free complete protease inhibitors) and disrupted by sonication for 5 minutes (BioRuptor, setting low) after one freeze/thaw cycle. Nuclei and cell debris were removed by centrifuging at 3,500 rpm for 5 minutes. The extracts were adjusted to

3 ml with FBB and mixed with 3 ml 1.08 M sucrose solution in FBB. This mixture was subsequently overlayed with 2 ml 0.27 M sucrose in FBB, 2 ml 0.135 M sucrose in FBB and 2 ml FBB only in SW41 polyallomer ultracentrifuge tubes (Beckman scientific) and spun for 1 hour 45 minutes at 30,000 rpm and 4℃. The fat cake was harvested by cutting with a tube slicer (Beckman scientific) and a cytosolic fraction was collected from the lower third portion of the gradient. The microsomal pellet was collected by resuspension in SDS-sample buffer without Bromphenol Blue in PBS. Proteins of the different fractions were delipidated and precipitated by methanol/chloroform precipitation. Protein pellets were dried by vacuum centrifugation and resuspended in SDS-sample buffer lacking Bromphenol Blue. Protein concentrations were measured with the RC/DC protein assay (Bio-Rad) and equal amounts were loaded on SDS-PAGE gels to allow western blot analysis. Since the LD fraction of unfed cells was basically devoid of proteins, we precipitated the complete fraction of the unfed and fed cell gradient top layer and loaded 20 μl each for comparison.

The following primary antibodies/sera were used: mouse anti-β-Tubulin E7 (dil. 1:2,000; DSHB), rat anti-CG9186 (dil. 1:3,000; this study), rabbit anti-PLIN2 (dil. 1:3,000; Grönke et al., 2003). Primary antibodies were combined with anti-mouse HRP (dil. 1:40,000, Pierce), anti-rabbit HRP (dil. 1:40,000, Pierce), anti-rat HRP (dil. 1:20,000; Jackson Immuno Research). Signals were detected by the Pierce Super Signal West Pico substrate (Pierce) in combination with a Fuji LAS-1000 imager equipped with an intelligent dark box II and the Fuji ImageGauge software.

Molecular modeling of the CG9186 structure and secondary structure analysis

The Protein homology/analogy Recognition Engine V 2.0 [Phyre2 (Kelley and Sternberg, 2009)] was used for homology modeling of CG9186. The first three highest scoring templates were epoxide hydrolases (PDB-IDs 1CR6, 2CJP, 2E3J). The resulting 3D model encompasses residue Met1 to Val307 and was depicted using Pymol (The PyMOL Molecular Graphics System, Version 1.4.1 Schrödinger, LLC.; http://www.pymol.org/).

Sequence analysis and secondary structure predictions

Helical wheel plots were generated using the software provided at http://rzlab.ucr.edu/scripts/wheel/wheel.cgi. Secondary structure predictions were performed with the NPS@ server (Combet et al., 2000) and hydrophobicity was analyzed with the ProtScale software (Gasteiger et al., 2005). All tools were used with the standard settings.

Tests for enzymatic activity of CG9186 and MGI:1916082
Preparation of COS-7 cell lysates

Two days after transfection, cells were washed with PBS, harvested with a cell scraper and disrupted by sonication in a solution containing 0.25 M sucrose, 1 mM DTT, 1 mM EDTA, 20 μg/ml leupeptin, 2 μg/ml antipain and 1 μg/ml pepstatin. Cell debris and nuclei were removed by centrifugation at 1,000 *g* for 5 minutes and protein concentration was determined according to Bradford (Bio-Rad). As a positive control we used a construct expressing the murine hormone-sensitive lipase as previously described (Lass et al., 2006).

Triacylglycerol hydrolase assay

The determination of triacylglycerol hydrolase activities in lysates of COS-7 cells was performed as described (Schweiger et al., 2006). Trioleoylglycerol (final concentration 0.33 mM) containing 0.03 μCi/nmol glycerol tri[9,10(n)-^{3}H]oleate as tracer was emulsified in a mixture of 45 μM phosphatidylcholine and phosphatidylinositol in 100 mM potassium phosphate buffer pH 7 with 2% defatted BSA by sonication on ice. 100 μl of COS-7 cell lysates containing 50 μg of protein were incubated with 100 μl of substrate in a water bath at 37℃ for 1 hour. The reactions were stopped by the addition of 3.25 ml methanol:chloroform:heptane (10:9:7) and 1 ml of 0.1 M potassium carbonate buffer pH 10.5. Fatty acids were extracted into the upper phase and radioactivity was determined by liquid scintillation counting.

Diacylglycerol hydrolase assay

The determination of diacylglycerol hydrolase activities was performed by incubating 100 μl of COS-7 cell lysates containing 50 μg protein with 100 μl of racemic dioleoylglycerol in a water bath at 37℃ for 1 hour. The substrate was prepared by emulsifying a dioleoylglycerol mixture (Sigma; final concentration 0.3 mM) with phosphatidylcholine (final concentration 50 μM) by sonication in 100 mM potassium phosphate buffer pH 7 containing 2% defatted BSA. The generation of free fatty acids was determined with a colorimetric kit (Wako) according to the manufacturer's instructions.

Monoacylglycerol hydrolase assay

The determination of monoacylglycerol hydrolase activities in COS-7 cell lysates was performed as described previously (Heier et al., 2010) using racemic 1,3-monooleoylglycerol (Sigma) as substrate and 20 μg of protein per assay.

Statistical analysis

Data are presented as means + s.d. Statistically significant differences between two groups were determined by unpaired Student's two-tailed t-tests. The following levels of statistical significance were used: n.s. not significant, $*P<0.05$; $**P<0.01$, $***P<0.001$.

Author contributions

M.B. conceived and supervised the project. M.B., A.L., H.J. and M.O. designed experiments, analyzed and interpreted the data, and wrote the manuscript. The molecular modeling of CG9186 was carried out by M.O. The other experiments were carried out by K.T., C.H., V.H. and P.J.T.

Supplementary material available online at
http://jcs.biologists.org/lookup/suppl/doi:10.1242/jcs.120493/-/DC1

References

Beckendorf, S. K. and Kafatos, F. C. (1976). Differentiation in the salivary glands of Drosophila melanogaster: characterization of the glue proteins and their developmental appearance. *Cell* **9**, 365-373.

Bell, M., Wang, H., Chen, H., McLenithan, J. C., Gong, D. W., Yang, R. Z., Yu, D., Fried, S. K., Quon, M. J., Londos, C. et al. (2008). Consequences of lipid droplet coat protein downregulation in liver cells: abnormal lipid droplet metabolism and induction of insulin resistance. *Diabetes* **57**, 2037-2045.

Beller, M., Riedel, D., Jänsch, L., Dieterich, G., Wehland, J., Jäckle, H. and Kühnlein, R. P. (2006). Characterization of the Drosophila lipid droplet subproteome. *Mol. Cell Proteomics* **5**, 1082-1094.

Beller, M., Sztalryd, C., Southall, N., Bell, M., Jäckle, H., Auld, D. S. and Oliver, B. (2008). COPI complex is a regulator of lipid homeostasis. *PLoS Biol.* **6**, e292.

Beller, M., Bulankina, A. V., Hsiao, H. H., Urlaub, H., Jäckle, H. and Kühnlein, R. P. (2010). PERILIPIN-dependent control of lipid droplet structure and fat storage in Drosophila. *Cell Metab.* **12**, 521-532.

Bickel, P. E., Tansey, J. T. and Welte, M. A. (2009). PAT proteins, an ancient family of lipid droplet proteins that regulate cellular lipid stores. *Biochim. Biophys. Acta* **1791**, 419-440.

Borgese, N. and Fasana, E. (2011). Targeting pathways of C-tail-anchored proteins. *Biochim. Biophys. Acta* **1808**, 937-946.

Boström, P., Andersson, L., Rutberg, M., Perman, J., Lidberg, U., Johansson, B. R., Fernandez-Rodriguez, J., Ericson, J., Nilsson, T., Borén, J. et al. (2007). SNARE proteins mediate fusion between cytosolic lipid droplets and are implicated in insulin sensitivity. *Nat. Cell Biol.* **9**, 1286-1293.

Boulant, S., Douglas, M. W., Moody, L., Budkowska, A., Targett-Adams, P. and McLauchlan, J. (2008). Hepatitis C virus core protein induces lipid droplet redistribution in a microtubule- and dynein-dependent manner. *Traffic* **9**, 1268-1282.

Brand, A. H. and Perrimon, N. (1993). Targeted gene expression as a means of altering cell fates and generating dominant phenotypes. *Development* **118**, 401-415.

Carvalho, M., Sampaio, J. L., Palm, W., Brankatschk, M., Eaton, S. and Shevchenko, A. (2012). Effects of diet and development on the Drosophila lipidome. *Mol. Syst. Biol.* **8**, 600.

Celniker, S. E., Dillon, L. A. L., Gerstein, M. B., Gunsalus, K. C., Henikoff, S., Karpen, G. H., Kellis, M., Lai, E. C., Lieb, J. D., MacAlpine, D. M. et al.; modENCODE Consortium (2009). Unlocking the secrets of the genome. *Nature* **459**, 927-930.

Cermelli, S., Guo, Y., Gross, S. P. and Welte, M. A. (2006). The lipid-droplet proteome reveals that droplets are a protein-storage depot. *Curr. Biol.* **16**, 1783-1795.

Chintapalli, V. R., Wang, J. and Dow, J. A. T. (2007). Using FlyAtlas to identify better Drosophila melanogaster models of human disease. *Nat. Genet.* **39**, 715-720.

Christianson, J. L., Boutet, E., Puri, V., Chawla, A. and Czech, M. P. (2010). Identification of the lipid droplet targeting domain of the Cidea protein. *J. Lipid Res.* **51**, 3455-3462.

Combet, C., Blanchet, C., Geourjon, C. and Deléage, G. (2000). NPS@: network protein sequence analysis. *Trends Biochem. Sci.* **25**, 147-150.

Depla, M., Uzbekov, R., Hourioux, C., Blanchard, E., Le Gouge, A., Gillet, L. and Roingeard, P. (2010). Ultrastructural and quantitative analysis of the lipid droplet clustering induced by hepatitis C virus core protein. *Cell Mol. Life Sci.* **67**, 3151-3161.

Dietzl, G., Chen, D., Schnorrer, F., Su, K.-C., Barinova, Y., Fellner, M., Gasser, B., Kinsey, K., Oppel, S., Scheiblauer, S. et al. (2007). A genome-wide transgenic RNAi library for conditional gene inactivation in Drosophila. *Nature* **448**, 151-156.

Digel, M., Ehehalt, R., Stremmel, W. and Füllekrug, J. (2009). Acyl-CoA synthetases: fatty acid uptake and metabolic channeling. *Mol. Cell. Biochem.* **326**, 23-28.

Farese, R. V., Jr and Walther, T. C. (2009). Lipid droplets finally get a little R-E-S-P-E-C-T. *Cell* **139**, 855-860.

Fei, W., Shui, G., Gaeta, B., Du, X., Kuerschner, L., Li, P., Brown, A. J., Wenk, M. R., Parton, R. G. and Yang, H. (2008). Fld1p, a functional homologue of human seipin, regulates the size of lipid droplets in yeast. *J. Cell Biol.* **180**, 473-482.

Fei, W., Shui, G., Zhang, Y., Krahmer, N., Ferguson, C., Kapterian, T. S., Lin, R. C., Dawes, I. W., Brown, A. J., Li, P. et al. (2011a). A role for phosphatidic acid in the formation of "supersized" lipid droplets. *PLoS Genet.* **7**, e1002201.

Fei, W., Li, H., Shui, G., Kapterian, T. S., Bielby, C., Du, X., Brown, A. J., Li, P., Wenk, M. R., Liu, P. et al. (2011b). Molecular characterization of seipin and its mutants: implications for seipin in triacylglycerol synthesis. *J. Lipid Res.* **52**, 2136-2147.

Fox, R. M., Hanlon, C. D. and Andrew, D. J. (2010). The CrebA/Creb3-like transcription factors are major and direct regulators of secretory capacity. *J. Cell Biol.* **191**, 479-492.

Fraenkel, G. and Brookes, V. J. (1953). The process by which the puparia of many species of flies become fixed to a substrate. *Biol. Bull.* **105**, 442-449.

Garcia, A., Sekowski, A., Subramanian, V. and Brasaemle, D. L. (2003). The central domain is required to target and anchor perilipin A to lipid droplets. *J. Biol. Chem.* **278**, 625-635.

Gasteiger, E., Hoogland, C., Gattiker, A., Duvaud, S., Wilkins, M. R., Appel, R. D. and Bairoch, A. (2005). Protein identification and analysis tools on the ExPASy server. In *The Proteomics Protocols Handbook* (ed. J. M. Walker), pp. 561-607. Totowa, NJ: Humana Press.

Gong, J., Sun, Z., Wu, L., Xu, W., Schieber, N., Xu, D., Shui, G., Yang, H., Parton, R. G. and Li, P. (2011). Fsp27 promotes lipid droplet growth by lipid exchange and transfer at lipid droplet contact sites. *J. Cell Biol.* **195**, 953-963.

Grandl, M. and Schmitz, G. (2010). Fluorescent high-content imaging allows the discrimination and quantitation of E-LDL-induced lipid droplets and Ox-LDL-generated phospholipidosis in human macrophages. *Cytometry A* **77**, 231-242.

Grönke, S., Beller, M., Fellert, S., Ramakrishnan, H., Jäckle, H. and Kühnlein, R. P. (2003). Control of fat storage by a Drosophila PAT domain protein. *Curr. Biol.* **13**, 603-606.

Grönke, S., Mildner, A., Fellert, S., Tennagels, N., Petry, S., Müller, G., Jäckle, H. and Kühnlein, R. P. (2005). Brummer lipase is an evolutionary conserved fat storage regulator in Drosophila. *Cell Metab.* **1**, 323-330.

Guo, Y., Walther, T. C., Rao, M., Stuurman, N., Goshima, G., Terayama, K., Wong, J. S., Vale, R. D., Walter, P. and Farese, R. V. (2008). Functional genomic screen reveals genes involved in lipid-droplet formation and utilization. *Nature* **453**, 657-661.

Hänisch, J., Wältermann, M., Robenek, H. and Steinbüchel, A. (2006). Eukaryotic lipid body proteins in oleogenous actinomycetes and their targeting to intracellular triacylglycerol inclusions: Impact on models of lipid body biogenesis. *Appl. Environ. Microbiol.* **72**, 6743-6750.

Harrod, M. J. and Kastritsis, C. D. (1972). Developmental studies in Drosophila. II. Ultrastructural analysis of the salivary glands of Drosophila pseudoobscura during some stages of development. *J. Ultrastruct. Res.* **38**, 482-499.

Heier, C., Taschler, U., Rengachari, S., Oberer, M., Wolinski, H., Natter, K., Kohlwein, S. D., Leber, R. and Zimmermann, R. (2010). Identification of Yju3p as functional orthologue of mammalian monoglyceride lipase in the yeast Saccharomycescerevisiae. *Biochim. Biophys. Acta.* **9**, 1063-1071.

Hildebrandt, A., Bickmeyer, I. and Kühnlein, R. P. (2011). Reliable Drosophila body fat quantification by a coupled colorimetric assay. *PLoS ONE* **6**, e23796.

Hinson, E. R. and Cresswell, P. (2009). The antiviral protein, viperin, localizes to lipid droplets via its N-terminal amphipathic alpha-helix. *Proc. Natl. Acad. Sci. USA* **106**, 20452-20457.

Horiguchi, Y., Araki, M. and Motojima, K. (2008). Identification and characterization of the ER/lipid droplet-targeting sequence in 17beta-hydroxysteroid dehydrogenase type 11. *Arch. Biochem. Biophys.* **479**, 121-130.

Hynynen, R., Suchanek, M., Spandl, J., Bäck, N., Thiele, C. and Olkkonen, V. M. (2009). OSBP-related protein 2 is a sterol receptor on lipid droplets that regulates the metabolism of neutral lipids. *J. Lipid Res.* **50**, 1305-1315.

Jaeger, K. E., Dijkstra, B. W. and Reetz, M. T. (1999). Bacterial biocatalysts: molecular biology, three-dimensional structures, and biotechnological applications of lipases. *Annu. Rev. Microbiol.* **53**, 315-351.

Jambunathan, S., Yin, J., Khan, W., Tamori, Y. and Puri, V. (2011). FSP27 promotes lipid droplet clustering and then fusion to regulate triglyceride accumulation. *PLoS ONE* **6**, e28614.

Kelley, L. A. and Sternberg, M. J. E. (2009). Protein structure prediction on the Web: a case study using the Phyre server. *Nat. Protoc.* **4**, 363-371.

Kienesberger, P. C., Lass, A., Preiss-Landl, K., Wolinski, H., Kohlwein, S. D., Zimmermann, R. and Zechner, R. (2008). Identification of an insulin-regulated lysophospholipase with homology to neuropathy target esterase. *J. Biol. Chem.* **283**, 5908-5917.

Kimmel, A. R., Brasaemle, D. L., McAndrews-Hill, M., Sztalryd, C. and Londos, C. (2010). Adoption of PERILIPIN as a unifying nomenclature for the mammalian PAT-family of intracellular lipid storage droplet proteins. *J. Lipid Res.* **51**, 468-471.

Krahmer, N., Guo, Y., Wilfling, F., Hilger, M., Lingrell, S., Heger, K., Newman, H. W., Schmidt-Supprian, M., Vance, D. E., Mann, M. et al. (2011). Phosphatidylcholine synthesis for lipid droplet expansion is mediated by localized activation of CTP:phosphocholine cytidylyltransferase. *Cell Metab.* **14**, 504-515.

Kuerschner, L., Moessinger, C. and Thiele, C. (2008). Imaging of lipid biosynthesis: how a neutral lipid enters lipid droplets. *Traffic* **9**, 338-352.

Kyte, J. and Doolittle, R. F. (1982). A simple method for displaying the hydropathic character of a protein. *J. Mol. Biol.* **157**, 105-132.

Lass, A., Zimmermann, R., Haemmerle, G., Riederer, M., Schoiswohl, G., Schweiger, M., Kienesberger, P., Strauss, J. G., Gorkiewicz, G. and Zechner, R. (2006). Adipose triglyceride lipase-mediated lipolysis of cellular fat stores is activated by CGI-58 and defective in Chanarin-Dorfman Syndrome. *Cell Metab.* **3**, 309-319.

Magré, J., Delépine, M., Khallouf, E., Gedde-Dahl, T., Jr, Van Maldergem, L., Sobel, E., Papp, J., Meier, M., Mégarbané, A., Bachy, A. et al.; BSCL Working Group (2001). Identification of the gene altered in Berardinelli-Seip congenital lipodystrophy on chromosome 11q13. *Nat. Genet.* **28**, 365-370.

McQuilton, P., St Pierre, S. E., Thurmond, J.; FlyBase Consortium (2012). FlyBase 101—the basics of navigating FlyBase. *Nucleic Acids Res.* **40 Database issue**, D706-D714.

Murphy, S., Martin, S. and Parton, R. G. (2010). Quantitative analysis of lipid droplet fusion: inefficient steady state fusion but rapid stimulation by chemical fusogens. *PLoS ONE* **5**, e15030.

Nishino, N., Tamori, Y., Tateya, S., Kawaguchi, T., Shibakusa, T., Mizunoya, W., Inoue, K., Kitazawa, R., Kitazawa, S., Matsuki, Y. et al. (2008). FSP27 contributes to efficient energy storage in murine white adipocytes by promoting the formation of unilocular lipid droplets. *J. Clin. Invest.* **118**, 2808-2821.

Schweiger, M., Schreiber, R., Haemmerle, G., Lass, A., Fledelius, C., Jacobsen, P., Tornqvist, H., Zechner, R. and Zimmermann, R. (2006). Adipose triglyceride lipase and hormone-sensitive lipase are the major enzymes in adipose tissue triacylglycerol catabolism. *J. Biol. Chem.* **52**, 40236-40241.

Subramanian, V., Garcia, A., Sekowski, A. and Brasaemle, D. L. (2004). Hydrophobic sequences target and anchor perilipin A to lipid droplets. *J. Lipid Res.* **45**, 1983-1991.

Szymanski, K. M., Binns, D., Bartz, R., Grishin, N. V., Li, W. P., Agarwal, A. K., Garg, A., Anderson, R. G. W. and Goodman, J. M. (2007). The lipodystrophy protein seipin is found at endoplasmic reticulum lipid droplet junctions and is important for droplet morphology. *Proc. Natl. Acad. Sci. USA* **104**, 20890-20895.

Taschler, U., Radner, F. P. W., Heier, C., Schreiber, R., Schweiger, M., Schoiswohl, G., Preiss-Landl, K., Jaeger, D., Reiter, B., Koefeler, H. C. et al. (2011). Monoglyceride lipase deficiency in mice impairs lipolysis and attenuates diet-induced insulin resistance. *J. Biol. Chem.* **286**, 17467-17477.

Teixeira, L., Rabouille, C., Rørth, P., Ephrussi, A. and Vanzo, N. F. (2003). Drosophila Perilipin/ADRP homologue Lsd2 regulates lipid metabolism. *Mech. Dev.* **120**, 1071-1081.

Tian, Y., Bi, J., Shui, G., Liu, Z., Xiang, Y., Liu, Y., Wenk, M. R., Yang, H. and Huang, X. (2011). Tissue-autonomous function of Drosophila seipin in preventing ectopic lipid droplet formation. *PLoS Genet.* **7**, e1001364.

Velikkakath, A. K. G., Nishimura, T., Oita, E., Ishihara, N. and Mizushima, N. (2012). Mammalian Atg2 proteins are essential for autophagosome formation and important for regulation of size and distribution of lipid droplets. *Mol. Biol. Cell* **23**, 896-909.

Welte, M. A., Cermelli, S., Griner, J., Viera, A., Guo, Y., Kim, D.-H., Gindhart, J. G. and Gross, S. P. (2005). Regulation of lipid-droplet transport by the perilipin homolog LSD2. *Curr. Biol.* **15**, 1266-1275.

Yang, H., Galea, A., Sytnyk, V. and Crossley, M. (2012). Controlling the size of lipid droplets: lipid and protein factors. *Curr. Opin. Cell Biol.* **24**, 509-516.

Yu, Y. V., Li, Z., Rizzo, N. P., Einstein, J. and Welte, M. A. (2011). Targeting the motor regulator Klar to lipid droplets. *BMC Cell Biol.* **12**, doi:10.1186/1471-2121-12-9.

Zehmer, J. K., Bartz, R., Bisel, B., Liu, P., Seemann, J. and Anderson, R. G. W. (2009). Targeting sequences of UBXD8 and AAM-B reveal that the ER has a direct role in the emergence and regression of lipid droplets. *J. Cell Sci.* **122**, 3694-3702.
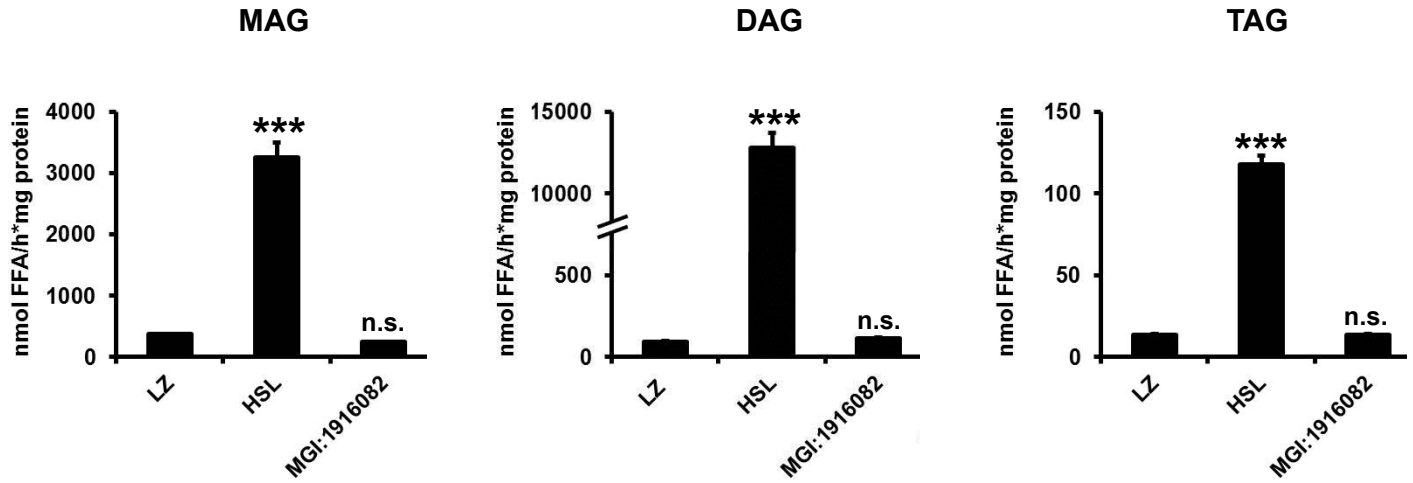
Fig. S1. Lipolytic activity towards trioleoylglycerol (TAG), dioleoylglycerol (DAG) or monooleoylglycerol (MAG) of COS-7 cells transiently transfected with constructs expressing β-gal (LZ), hormone sensitive lipase (HSL) or MGI:1916082. Please note that the β-gal and HSL measurements are identical with the ones shown in Fig. 5G.
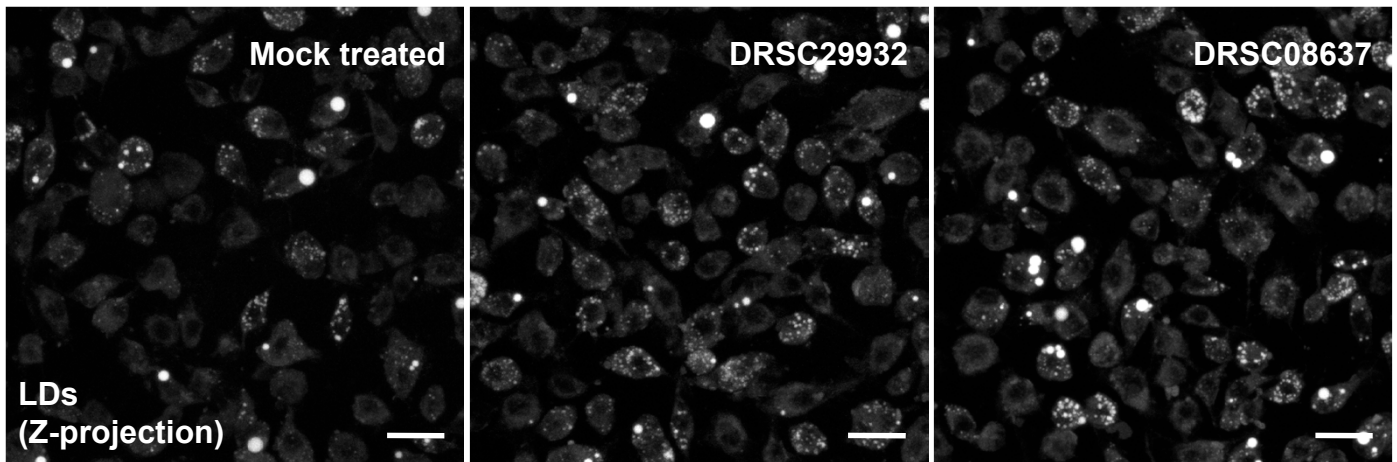
Fig. S2. *Drosophila* Kc167 cells incubated with 400 μM OA were mock treated or incubated with dsRNAs targeting CG9186-encoding transcripts (DRSC29932 or DRSC08637) for six days. LDs were visualized by BODIPY493/503. The knockdown of CG9186 in the tissue culture cells has no clear-cut effect on storage lipid levels. Scale bars: 15 μm.
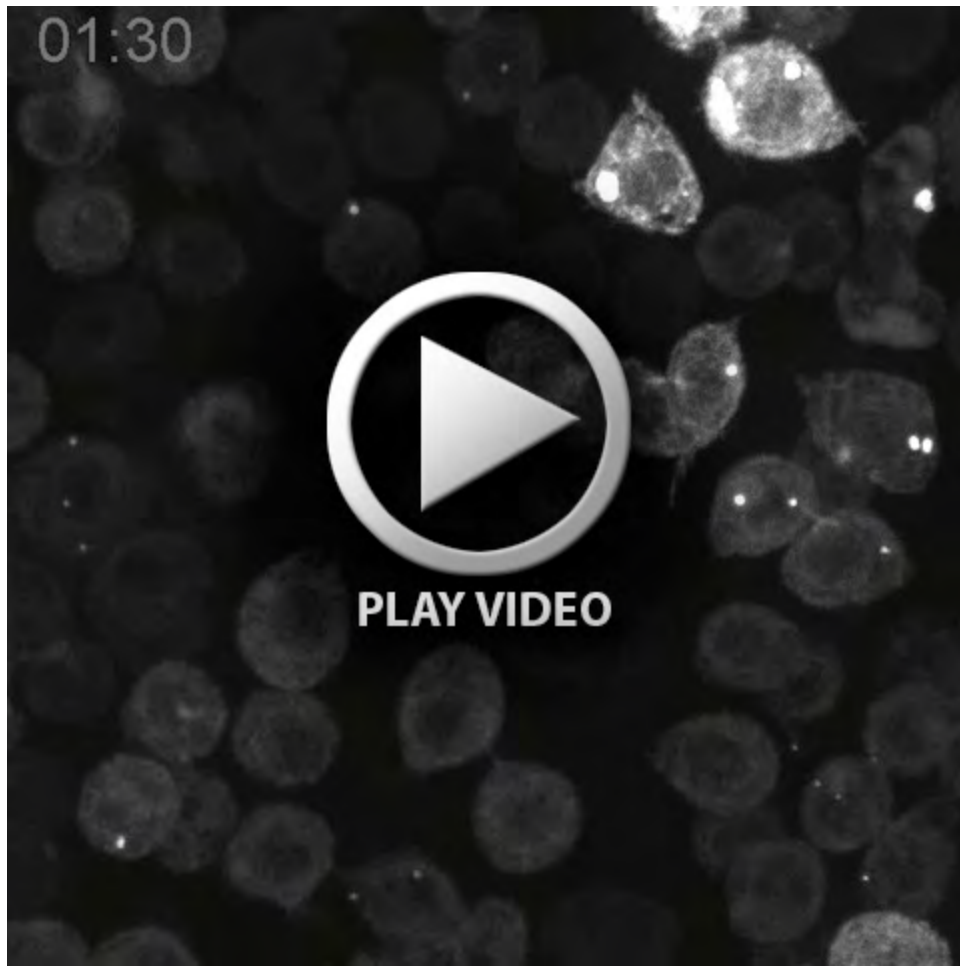
Movie 1. Time-lapse movie of CG9186 expressing cells incubated in the presence of oleic acid to induce lipid droplets.